

Synthesis, Structures, and Luminescence Behavior of Mixed Metal Alkynyl Platinum–Cadmium Complexes[§]

Julio Fernández,[†] Juan Forniés,^{*‡} Belén Gil,[†] Julio Gómez,[†] Elena Lalinde^{*†} and M. Teresa Moreno[†]

Departamento de Química-Grupo de Síntesis Química de La Rioja, UA-CSIC, Universidad de La Rioja, 26006, Logroño, Spain, and Departamento de Química Inorgánica, Instituto de Ciencia de Materiales de Aragón, Universidad de Zaragoza-Consejo Superior de Investigaciones Científicas, 50009 Zaragoza, Spain

Received December 26, 2005

This article describes the preparation, characterization, and optical properties of new bi- and trinuclear tweezer-type platinum cadmium derivatives, stabilized by η^2 -alkyne–cadmium bonding. Treatment of $Q_2[*cis*-Pt(C_6F_5)_2(C\equiv CR)_2]$ (**1a–1c**) with $CdCl_2 \cdot 2.5 H_2O$ (1:1) produces dinuclear Pt–Cd adducts $Q_2-[\{*cis*-Pt(C_6F_5)_2(\mu-\kappa C^\alpha:\eta^2-C\equiv CR)_2\}(CdCl_2)]$ ($Q = NBu_4$, $R = t-Bu$ **2a**; $Q = PMePh_3$, $R = Ph$ **2b**; $R = Tol$ **2c**). However, reaction of $(NBu_4)_2[*cis*-Pt(C_6F_5)_2(C\equiv CR)_2]$ with $Cd(NO_3)_2 \cdot 4H_2O$ produces trinuclear Pt_2Cd dianionic complexes $(NBu_4)_2[\{*cis*-Pt(C_6F_5)_2(\mu-\kappa C^\alpha:\eta^2-C\equiv CR)_2\}_2Cd]$ (**3a–3c**). The analogous $(PMePh_3)_2[\{*cis*-Pt(C_6F_5)_2(\mu-\kappa C^\alpha:\eta^2-C\equiv CR)_2\}_2Cd]$ ($R = Ph$ **3b'**; Tol **3c'**) were prepared similarly starting from $(PMePh_3)_2[*cis*-Pt(C_6F_5)_2(C\equiv CR)_2]$. The crystal structures of **2c** and **3a,b** show that the cadmium center is well embedded by the *cis*-bis(alkyne)platinate entities, leading to planar PtC_4Cd cores. In the heterometallic species, the low-energy absorption, which is ascribed to an admixture of $\pi \rightarrow \pi^*(C\equiv CR)$ $IL/d\pi(Pt) \rightarrow \pi^*(C\equiv CR)$ MLCT, exhibits a clear hypsochromic shift compared to its precursors, probably due to the existence of a lesser delocalization on the alkynyl fragments upon the η^2 -complexation. The arylalkynyl derivatives (**b**, **c**) display intense structured emission bands, arising from ${}^3\pi\pi^*(C\equiv CR)$ (IL) and/or mixed ${}^3\pi\pi^*/Pt(d_\pi)(C\equiv CR) \rightarrow \pi^*(C\equiv CR)$ (3MLCT) manifolds with a predominant IL character.

Introduction

Alkynyl complexes have been actively investigated for many years.^{1–16} Their interest mainly lies in (i) the ability of the alkynyl group to bind to transition metals, forming polynuclear complexes displaying an unusually rich variety of structures, and (ii) the versatile reactivity of the coordinated alkynyl ligand, which is employed as an adequate strategy for the synthesis of

other target carbon-rich organometallic compounds. Interest in these systems has also been stimulated by their rich electronic and luminescent properties and potential applications in molecular electronics.^{17–19} However, in contrast to the large body of work on the luminescent properties of σ -bonded alkynyl complexes,^{20–33} luminescence studies of related π -bonded systems are relatively sparse.^{34–44} In this context, we^{45–51} and others^{34–44} have shown the possibility and feasibility of tuning

[§] Dedicated to our friend Dr. Jose Antonio Abad on the occasion of his retirement.

* Corresponding authors. E-mail: elena.lalinde@dq.unirioja.es. Fax: (+34) 941-299-621. E-mail: juan.fornies@unizar.es. Fax: (+34) 976-761-187.

[†] Universidad de La Rioja, UA-CSIC

[‡] Universidad de Zaragoza-CSIC.

(1) Nast, R. *Coord. Chem. Rev.* **1982**, *47*, 89.

(2) Beck, W.; Niemer, B.; Wiesser, M. *Angew. Chem., Int. Ed. Engl.* **1993**, *32*, 923.

(3) Lotz, S.; Van Rooyen, P. H.; Meyer, R. *Adv. Organomet. Chem.* **1995**, *37*, 219.

(4) Manna, J.; John, K. D.; Hopkins, H. D. *Adv. Organomet. Chem.* **1995**, *38*, 79.

(5) Forniés, J.; Lalinde, E. *J. Chem. Soc., Dalton Trans.* **1996**, 2587.

(6) Bruce, M. I. *Coord. Chem. Rev.* **1997**, *166*, 91.

(7) Belluco, U.; Bertani, R.; Michelin, R. A.; Mozzon, M. *J. Organomet. Chem.* **2000**, *600*, 37.

(8) Lang, H.; George, D. S. A.; Rheinwald, G. *Coord. Chem. Rev.* **2000**, *206–207*, 101.

(9) Choukroun, R.; Cassoux, P. *Acc. Chem. Res.* **1999**, *32*, 494.

(10) Long, N. J.; Williams, C. K. *Angew. Chem., Int. Ed.* **2003**, *42*, 2586.

(11) Low, P. J.; Bruce, M. I. *Adv. Organomet. Chem.* **2002**, *48*, 71.

(12) Rosenthal, U. *Angew. Chem., Int. Ed.* **2003**, *42*, 1794.

(13) Rigaut, S.; Touchard, D.; Dixneuf, P. H. *Coord. Chem. Rev.* **2004**, *248*, 1585.

(14) Selegue, J. P. *Coord. Chem. Rev.* **2004**, *248*, 1543.

(15) Cadierno, V.; Gamasa, M. P.; Gimeno, J. *Coord. Chem. Rev.* **2004**, *248*, 1627.

(16) Ruschewitz, U. *Coord. Chem. Rev.* **2003**, *244*, 115.

(17) Whittall, I. R.; McDonagh, A. M.; Humphrey, M. G.; Samoc, M. *Adv. Organomet. Chem.* **1998**, *43*, 349.

(18) Ziesel, R.; Hissler, M.; El-ghayoury, A.; Harriman, A. *Coord. Chem. Rev.* **1998**, *178–180*, 1251.

(19) Paul, F.; Lapinte, C. *Coord. Chem. Rev.* **1998**, *178–180*, 431.

(20) Yam, V. W. W. *J. Organomet. Chem.* **2004**, *689*, 1393.

(21) Yam, V. W. W.; Lo, W. Y.; Lam, C. H.; Fung, W. K. M.; Wong, K. M. C.; Lan, V. C. Y.; Zhu, N. *Coord. Chem. Rev.* **2003**, *245*, 39.

(22) Yam, V. W. W. *Chem. Commun.* **2001**, 789.

(23) Slageren, J. V.; Klein, A.; Zális, S. *Coord. Chem. Rev.* **2002**, *230*, 193.

(24) Pomestchenko, I. E.; Polyansky, D. E.; Castellano, F. N. *Inorg. Chem.* **2005**, *44*, 3412.

(25) Wadas, T. J.; Chakraborty, S.; Lachicotte, R. J.; Wang, Q. M.; Eisenberg, R. *Inorg. Chem.* **2005**, *44*, 2628.

(26) Zhao, X.; Cardolaccia, T.; Farley, R. T.; Abboud, K. A.; Schanze, K. S. *Inorg. Chem.* **2005**, *44*, 2619.

(27) Wong, K. M. C.; Tang, W. S.; Lu, X. X.; Zhu, N.; Yam, V. W. W. *Inorg. Chem.* **2005**, *44*, 1492.

(28) Tao, C. H.; Zhu, N.; Yam, V. W. W. *Chem. Eur. J.* **2005**, *11*, 1647.

(29) Hua, F.; Kynayyigit, S.; Cable, J. R.; Castellano, F. N. *Inorg. Chem.* **2005**, *44*, 471.

(30) Onitsuka, K.; Fujimoto, M.; Kitajima, H.; Ohshiro, N.; Takeji, F.; Takahashi, S. *Chem. Eur. J.* **2004**, *10*, 6433.

(31) Haskins-Glusac, K.; Pinto, M. R.; Tan, C.; Schanze, K. S. **2004**, *126*, 14964.

(32) Wei, Q. H.; Yin, G. Q.; Zhang, L. Y.; Shi, L. X.; Mao, Z. W.; Chen, Z. N. *Inorg. Chem.* **2004**, *43*, 3484.

(33) Chao, H. Y.; Lu, W.; Li, Y.; Chan, M. C. W.; Che, C. M.; Cheung, K. K.; Zhu, N. *J. Am. Chem. Soc.* **2002**, *124*, 14696.

the luminescence behavior of alkynyl complexes not only by perturbation of the electron density of the alkynyl ligands via η^2 -(M)-coordination but also through the occurrence of Pt \cdots Pt and/or Pt \cdots M bonding interactions. The versatile coordination of organometallic-substituted alkynes $L_nMC\equiv CR$ toward coinage d^{10} metals [Cu(I), Ag(I), Au(I)] and the alkynyl chemistry of these metals has been amply demonstrated.^{4,5,8,52–55} By contrast, the chemistry of group 12 metal alkynyls has not been thoroughly investigated,^{52,56–63} and research work into cadmium-(II) systems in particular is still in its beginnings.^{64–67} We have recently shown⁶⁸ that the homoleptic complex $(NBU_4)_2[Pt(C\equiv CPh)_4]$ reacts with $CdCl_2 \cdot 2.5H_2O$ (1:2 molar ratio) to afford the simple 1:2 adduct $(NBU_4)_2[Pt(C\equiv CPh)_4(CdCl_2)_2]$, containing unusual η^2 -alkyne Cd interactions, together with an unexpected,

(34) Yam, V. W. W. *Acc. Chem. Res.* **2002**, *35*, 555, and references therein.

(35) Yam, V. W. W.; Lo, K. K. W.; Wong, K. M. C. *J. Organomet. Chem.* **1999**, *578*, 3.

(36) Wong, K. M. C.; Hui, C. K.; Yu, K. L.; Yam, V. W. W. *Coord. Chem. Rev.* **2002**, *229*, 123.

(37) Ford, P. C.; Cariati, E.; Bourassa, J. *Chem. Rev.* **1999**, *99*, 3625.

(38) Wei, Q. H.; Zhang, L. Y.; Yin, G. Q.; Shi, L. X.; Cheng, Z. N. *J. Am. Chem. Soc.* **2004**, *126*, 9940.

(39) Higgs, T. C.; Parsons, S.; Bailey, P. J.; Jones, A. C.; MacLachlan, F.; Parkin, A.; Dawson, A.; Tasker, P. A. *Organometallics* **2002**, *21*, 5692.

(40) Yam, V. W. W.; Hui, C. K.; Yu, S. Y.; Zhu, N. *Inorg. Chem.* **2004**, *43*, 812.

(41) Wei, Q. H.; Yin, G. Q.; Ma, Z.; Shi, L. X.; Chen, Z. N. *Chem. Commun.* **2003**, 2188.

(42) Yam, V. W. W.; Cheung, K. L.; Cheng, E. C. C.; Zhu, N.; Cheung, K. K. *Dalton Trans.* **2003**, 1830.

(43) Yam, V. W. W.; Chong, S. H. F.; Wong, K. M. C.; Cheung, K. K. *Chem. Commun.* **1999**, 1013.

(44) Yam, V. W. W.; Fung, W. K. M.; Cheung, K. K. *Angew. Chem., Int. Ed. Engl.* **1996**, *35*, 1100.

(45) Ara, I.; Berenguer, J. R.; Forniés, J.; Gómez, J.; Lalinde, E.; Merino, R. I. *Inorg. Chem.* **1997**, *36*, 6461.

(46) Ara, I.; Forniés, J.; Gómez, J.; Lalinde, E.; Moreno, M. T. *Organometallics* **2000**, *19*, 3137.

(47) Charmant, J. P. H.; Forniés, J.; Gómez, J.; Lalinde, E.; Merino, R.; Moreno, M. T.; Orpen, A. G. *Organometallics* **1999**, *18*, 3353.

(48) Berenguer, J. R.; Forniés, J.; Gómez, J.; Lalinde, E.; Moreno, M. T. *Organometallics* **2001**, *20*, 4847, and references therein.

(49) Charmant, J. P. H.; Forniés, J.; Gómez, J.; Lalinde, E.; Merino, R. I.; Moreno, M. T.; Orpen, A. G. *Organometallics* **2003**, *22*, 652.

(50) Forniés, J.; Gómez, J.; Lalinde, E.; Moreno, M. T. *Inorg. Chim. Acta* **2003**, *347*, 145.

(51) Ara, I.; Berenguer, J. R.; Eguizábal, E.; Forniés, J.; Gómez, J.; Lalinde, E. *J. Organomet. Chem.* **2003**, *670*, 221.

(52) Mingos, D. M. P.; Vilar, R.; Rais, D. *J. Organomet. Chem.* **2002**, *641*, 126.

(53) Lang, H.; del Vilar, A. *J. Organomet. Chem.* **2003**, *670*, 45.

(54) Lang, H.; Stein, T. *J. Organomet. Chem.* **2002**, *641*, 41.

(55) Lang, H.; Köhler, K.; Blau, S. *Coord. Chem. Rev.* **1995**, *145*, 113.

(56) Liao, Y.; Feng, J. K.; Yang, L.; Reu, A. M.; Zhang, H. X. *Organometallics* **2005**, *24*, 385.

(57) Wong, W. Y.; Lu, G. L.; Lin, L.; Shi, J. X.; Lin, Z. *Eur. J. Inorg. Chem.* **2004**, 2066, and references therein.

(58) Rais, D.; Mingos, D. M. P.; Vilar, R.; White, A. J. P.; Williams, D. *J. Organometallics* **2000**, *19*, 5209.

(59) Wong, W. Y.; Choi, K. H.; Lu, G. L.; Lin, Z. *Organometallics* **2002**, *21*, 4475.

(60) Wong, W. Y.; Liu, L.; Shi, J. X. *Angew. Chem., Int. Ed.* **2003**, *42*, 4064.

(61) Wong, W. Y.; Choi, K. H.; Lu, G. L.; Shi, J. X.; Lai, P. Y.; Chan, S. M.; Lin, Z. *Organometallics* **2001**, *20*, 5446.

(62) Berenguer, J. R.; Forniés, J.; Lalinde, E.; Martín, A.; Moreno, M. T. *J. Chem. Soc., Dalton Trans.* **1994**, 3343.

(63) Zhang, D.; McConville, D. B.; Tessier, C. A.; Youngs, W. J. *Organometallics* **1997**, *16*, 824.

(64) Nast, R.; Richers, L. Z. *Angew. Chem.* **1963**, *319*, 320.

(65) Jeffery, E. A.; Mole, T. *J. Organomet. Chem.* **1968**, *11*, 393.

(66) Barr, D.; Edwards, A. J.; Raithby, P. R.; Rennie, M. A.; Verhoevert, K.; Wrich, D. S. *J. Chem. Soc., Chem. Commun.* **1994**, 1627.

(67) Forniés, J.; Ibañez, S.; Martín, A.; Gil, B.; Lalinde, E.; Moreno, M. T. *Organometallics* **2004**, *23*, 3963.

(68) Charmant, J. P. H.; Falvello, L. R.; Forniés, J.; Gómez, J.; Lalinde, E.; Moreno, M. T.; Orpen, A. G.; Rueda, A. *Chem. Commun.* **1999**, 2045.

strongly luminescent, tetranuclear cluster, $(NBU_4)_2[Pt(C\equiv CPh)_4]_2(CdCl_2)_2]$, stabilized by μ - η^1 alkynyl bridging ligands and Pt \cdots Cd bonding interactions (Pt–Cd 2.960(1) Å). The analogous reaction with $Cd(ClO_4)_2 \cdot 6H_2O$ evolves with formation of the expected neutral product $[PtCd(C\equiv CPh)_4]_n$, with an insoluble white solid of unknown structure together with yellow crystals of an unexpected decanuclear Pt(II)–Cd(II) cluster, $[Pt_4Cd_6(C\equiv CPh)_4(\mu-C\equiv CPh)_{12}(\mu_3-OH)_4]$.⁶⁹ Here we report the extension of these reactions to the heteroleptic anionic structures $[cis-Pt(C_6F_5)_2(C\equiv CR)_2]^{2-}$ (R = *t*-Bu, Ph, Tol), which have allowed us to prepare simple 1:1 dianionic adducts $[{cis-Pt(C_6F_5)_2(C\equiv CR)_2}CdCl_2]^{2-}$, together with very unusual trinuclear anions Pt_2Cd , $[{cis-Pt(C_6F_5)_2(C\equiv CR)_2}_2Cd]^{2-}$, formed by two orthogonal “Pt(C₆F₅)₂(C≡CR)₂” fragments acting as bidentate diyne ligands toward a Cd(II) ion, as confirmed by X-ray (R = *t*-Bu, Ph). To the best of our knowledge, these complexes are the first reported examples in which a cadmium center is stabilized only by η^2 -alkyne interactions. The luminescence properties of these binuclear Pt–Cd and trinuclear Pt₂Cd complexes have also been investigated.

Experimental Section

General Considerations. All reactions and manipulations were carried out under nitrogen atmosphere using Schlenk techniques and distilled solvents purified by known procedures. IR spectra were recorded on a Perkin-Elmer FT-IR 1000 spectrometer as Nujol mulls between polyethylene sheets. NMR spectra were recorded on Bruker ARX 300 and Bruker AVANCE 400 spectrometers, chemical shifts are reported in ppm relative to external standards (SiMe₄ and CFCl₃), and coupling constants are in Hz. Complexes **2** are not soluble enough to register the ¹³C{¹H} NMR spectra. Elemental analyses were carried out with a Perkin-Elmer 2400 CHNS/O microanalyzer and the electrospray mass spectra with a VG Autospec double-focusing mass spectrometer operating in the negative FAB mode or a HP5989B mass spectrometer with interphase API-ES HP 59987A. MALDI-TOF spectra were recorded in a Microflex MALDI-TOF Bruker spectrometer operating in the linear and reflector modes using dithranol as matrix. Conductivities were measured in acetone or acetonitrile solutions (ca. 5 × 10^{−4} mol L^{−1}) using a Crison GLP31 conductimeter. UV–visible spectra were obtained on a Hewlett-Packard 8453 spectrometer. Emission and excitation spectra were obtained on a Jobin-Yvon Horiba Fluorolog 3-11 Tau-3 spectrofluorimeter, in which the lifetime measurements were performed operating in the phosphorimeter mode. The precursors $Q_2[*cis*-Pt(C_6F_5)_2(C\equiv CR)_2]$ (R = *t*-Bu, Q = NBU₄, **1a**; R = Ph, Q = PMePh₃, **1b**)⁷⁰ were prepared according to reported procedures.

Synthesis of (PMePh₃)₂[*cis*-Pt(C₆F₅)₂(C≡CTol)₂], **1c.** [*cis*-Pt(C₆F₅)₂(tht)₂]⁷¹ (0.30 g, 0.425 mmol) was added to a fresh (−20 °C) solution of LiC≡CTol (2.125 mmol) in Et₂O (40 mL). The mixture was stirred at low temperature for 15 min and then was allowed to reach room temperature (ca. 30 min). The solvent was removed in a vacuum, and the residue was extracted with cold *i*-PrOH (~20 mL) and filtered through Celite. Treatment of the filtrate with [PMePh₃]Br (0.38 g, 1.06 mmol) caused the precipitation of **1c** as a white solid (0.40 g, 72% yield). Anal. Calcd for C₆₈F₁₀H₅₀P₂Pt (1314.16): C, 62.15; H, 3.83. Found: C, 62.02; H, 3.44. Λ_M (acetonitrile): 223.4 Ω^{−1}·cm²·mol^{−1}. MS FAB(−): *m/z* 644 ([Pt(C₆F₅)₂(C≡CTol)][−] 100%). IR (cm^{−1}): $\nu(C\equiv C)$ 2091s, 2078s; $\nu(C_6F_5)_{Xsens}$ 781m, 775m. ¹H NMR (CDCl₃, 20 °C, δ):

(69) Forniés, J.; Gómez, J.; Lalinde, E.; Moreno, M. T. *Inorg. Chem.* **2001**, *40*, 5415.

(70) Espinet, P.; Forniés, J.; Martínez, F.; Sotés, M.; Lalinde, E.; Moreno, M. T.; Ruiz, A.; Welch, A. J. *J. Organomet. Chem.* **1991**, *403*, 253.

(71) Usón, R.; Forniés, J.; Martínez, F.; Tomás, M. *J. Chem. Soc., Dalton Trans.* **1980**, 888.

7.77–7.13 (m, 34H, aromatics), 6.60 (m, 4H, aromatics), 3.77 [d, $^2J(\text{P-H}) = 12.2$ Hz, 6H, CH₃, PMePh₃], 2.12 (s, 6H, CH₃, Tol). ^{19}F NMR (CDCl₃, 20 °C, δ): -115.1 [dm, $^3J(\text{Pt-F}_o) = 378$ Hz, 4F_o], -167.8 (m, 2F_m), -168.8 (t, 2F_p). $^{13}\text{C}\{^1\text{H}\}$ NMR (CD₃COCD₃, -90 °C, δ): 147.9 [dd, $^1J(\text{C-F}) = 222$ Hz, $^2J(\text{C-F}) = 24$ Hz, C-F_o, C₆F₅], 135.5 [dm, $^1J(\text{C-F}) \approx 260$ Hz, C-F_m/F_p, C₆F₅], 134.9 (s, br, C_p, PMePh₃), 133.7 [d, $J(\text{C-P}) = 10.7$ Hz, Ph, PMePh₃], 131.7 (s, C⁴, Tol), 130.3 [d, $J(\text{C-P}) = 12.7$ Hz, Ph, PMePh₃], 130.1 (s, CH, Tol), 128.4 (s, CH, Tol), 128.2 (s, C¹, Tol), 120.5 (s, C_i, Tol), 120.0 [d, $J(\text{C-P}) = 88$ Hz, C_i, PMePh₃], 117.3 (s, br $^1J(\text{C-Pt}) = 1075$ Hz, C_α, C_α≡C_βPh], 103.7 [s, $^2J(\text{C-Pt}) = 308$ Hz, C_β, C_α≡C_βTol], 20.6 (s, CH₃, Tol), 7.7 [d, $J(\text{C-P}) = 56$ Hz, CH₃, PMePh₃].

Synthesis of (NBu₄)₂[*cis*-Pt(C₆F₅)₂(μ-κC^α:η²-C≡Ct-Bu)₂](CdCl₂)], **2a**. To a solution of (NBu₄)₂[*cis*-Pt(C₆F₅)₂(C≡Ct-Bu)₂] (0.150 g, 0.128 mmol) in acetone (25 mL) was added CdCl₂·2.5H₂O (0.029 g, 0.128 mmol), and the mixture was stirred for 1 h. Evaporation to small volume (~2 mL) and addition of 10 mL of *n*-hexane caused the precipitation of **2a** as a white solid, which was filtered, washed with *n*-hexane, and air-dried (0.138 g, 77% yield). Anal. Calcd for CdC₅₆Cl₂F₁₀H₉₀N₂Pt (1359.73): C, 49.47; H, 6.67; N, 2.06. Found: C, 49.32; H, 6.52; N, 2.03. Λ_M (acetone): 281 Ω⁻¹·cm²·mol⁻¹. MS FAB(-): *m/z* 1737 ([Pt₂(C₆F₅)₄(C≡Ct-Bu)₄Cd(NBu₄)₄]⁻ 4%), 856 ([Pt(C₆F₅)₂(C≡Ct-Bu)₂-CdCl(OH)]⁻ 69%), 839 ([Pt(C₆F₅)₂(C≡Ct-Bu)₂CdCl]⁻ 87%), 610 ([Pt(C₆F₅)₂(C≡Ct-Bu)]⁻ 71%), 529 ([Pt(C₆F₅)₂]⁻ 84%), 510 ([Pt(C₆F₅)CdCl]⁻ 90%), 362 ([Pt(C₆F₅)]⁻ 100%). IR (cm⁻¹): ν(C≡C) 2051m, 2022sh; ν(C₆F₅)_{Xsens} 787m, 778m; ν(Cd-Cl) 261br,m. ^1H NMR (CDCl₃, 20 °C, δ): 3.37 (m, 16H, NCH₂, NBu₄), 1.68 (m, 16H, CH₂, NBu₄), 1.38 (m, 16H, CH₂, NBu₄), 1.19 (s, 18H, *t*-Bu), 0.93 (t, 24H, CH₃, NBu₄). ^{19}F NMR (CDCl₃, 20 °C, δ): -115.6 [dm, $^3J(\text{Pt-F}_o) = 381$ Hz, 4F_o], -167.2 (m, 2F_p), -167.7 (m, 4F_m).

Synthesis of (PMePh₃)₂[*cis*-Pt(C₆F₅)₂(μ-κC^α:η²-C≡CPh)₂](CdCl₂)], **2b**. A solution of (PMePh₃)₂[*cis*-Pt(C₆F₅)₂(C≡CPh)₂] (0.150 g, 0.117 mmol) in acetone (15 mL) was treated with CdCl₂·2.5H₂O (0.027 g, 0.117 mmol). After 4 h of stirring, the mixture was filtered through Kieselguhr and evaporated to a small volume, giving a white solid **2b**, which was filtered off and washed with cold acetone (0.090 g, 53% yield). Anal. Calcd for CdC₆₆Cl₂F₁₀H₄₆P₂Pt (1469.10): C, 53.95; H, 3.16. Found: C, 53.62; H, 3.45%. Λ_M (acetone): 235 Ω⁻¹·cm²·mol⁻¹. MS FAB(-): *m/z* 1854 ([Pt₂(C₆F₅)₄(C≡CPh)₄CdCl(NBu₄)₄]⁻ 7%), 879 ([Pt(C₆F₅)₂(C≡CPh)₂-CdCl]⁻ 36%), 630 ([Pt(C₆F₅)₂(C≡CPh)]⁻ 73%), 564 ([Pt(C₆F₅)(C≡CPh)₂]⁻ 62%), 510 ([Pt(C₆F₅)CdCl]⁻ 100%), 362 ([Pt(C₆F₅)]⁻ 100%). IR (cm⁻¹): ν(C≡C) 2053m, 2042m; ν(C₆F₅)_{Xsens} 788m, 778w; ν(Cd-Cl) 288w, 275m. ^1H NMR (CDCl₃, 20 °C, δ): 7.72–7.13 (m, 40H, Ph, C≡CPh and PMePh₃), 3.65 [d, $^2J(\text{P-H}) = 12.8$ Hz, 6H, CH₃, PMePh₃]. ^{19}F NMR (CDCl₃, 20 °C, δ): -116.3 [d, $^3J(\text{Pt-F}_o) = 394$ Hz, 4F_o], -166.2 (t, 2F_p), -166.8 (m, 4F_m).

Synthesis of (PMePh₃)₂[*cis*-Pt(C₆F₅)₂(μ-κC^α:η²-C≡CTol)₂](CdCl₂)], **2c**. Compound **2c** (beige solid) was prepared following the same procedure as compound **2b**, but starting from (PMePh₃)₂[*cis*-Pt(C₆F₅)₂(C≡CTol)₂] (0.150 g, 0.114 mmol) and CdCl₂·2.5H₂O (0.023 g, 0.114 mmol) (0.145 g, 88% yield). Anal. Calcd for CdC₆₈Cl₂F₁₀H₅₀P₂Pt (1497.47): C, 54.54; H, 3.37. Found: C, 54.34; H, 3.80. Λ_M (acetonitrile): 223.4 Ω⁻¹·cm²·mol⁻¹. MS ES(-): *m/z* 760 ([Pt(C₆F₅)₂(C≡CTol)₂ + H]⁻ 50%), 696 ([Pt(C₆F₅)₂]⁻ 51%), 644 ([Pt(C₆F₅)₂(C≡CTol)]⁻ 100%). IR (cm⁻¹): ν(C≡C) 2063s, 2055sh; ν(C₆F₅)_{Xsens} 789s, 781s; ν(Cd-Cl) 277m, 269sh. ^1H NMR (CD₃COCD₃, 20 °C, δ): 7.62, 7.49 (m, 30H, Ph, PMePh₃), 7.30 (d, $J = 7.8$ Hz, 4H, C₆H₄, Tol), 6.92 (d, $J = 7.8$ Hz, 4H, C₆H₄, Tol), 3.65 [d, $^2J(\text{P-H}) = 12.8$ Hz, 6H, CH₃, PMePh₃], 2.21 (s, 6H, CH₃, Tol). ^{19}F NMR (CD₃COCD₃, 20 °C, δ): -116.2 [dm, $^3J(\text{Pt-F}_o) = 396$ Hz, 4F_o], -166.5 (t, 2F_p), -166.9 (m, 4F_m).

Synthesis of (NBu₄)₂[*cis*-Pt(C₆F₅)₂(μ-κC^α:η²-C≡Ct-Bu)₂]₂Cd], **3a**. A solution of (NBu₄)₂[*cis*-Pt(C₆F₅)₂(C≡Ct-Bu)₂] (0.125 g, 0.106

mmol) in acetone (20 mL) was treated with Cd(NO₃)₂·4H₂O (0.016 g, 0.053 mmol), and after 1.5 h of stirring, the mixture was filtered through Kieselguhr and evaporated to dryness. The white residue was treated with cold *i*-PrOH (~5 mL), giving a white solid, **3a**, which was filtered off and washed with cold *i*-PrOH (0.070 g, 67% yield). Anal. Calcd for CdC₈₀F₂₀H₁₀₈N₂Pt₂ (1980.30): C, 48.52; H, 5.50; N, 1.42. Found: C, 48.22; H, 5.54; N, 1.18. Λ_M (acetonitrile): 231 Ω⁻¹·cm²·mol⁻¹. MALDI-TOF (-): *m/z* 1738 ([M + NBu₄]⁻ 8%), 610 ([Pt(C₆F₅)₂(C≡Ct-Bu)]⁻ 100%). IR (cm⁻¹): ν(C≡C) 2053s; ν(C₆F₅)_{Xsens} 805sh, 789s, 777s. ^1H NMR (CD₃COCD₃, 20 °C, δ): 3.46 (m, 16H, NCH₂, NBu₄), 1.84 (m, 16H, CH₂, NBu₄), 1.43 (m, 16H, CH₂, NBu₄), 1.37 (s, 36H, *t*-Bu), 0.98 (t, 24H, CH₃, NBu₄). ^{19}F NMR (CDCl₃, 20 °C, δ): -114.5 [dm, $^3J(\text{Pt-F}_o) = 420$ Hz; 8F_o], -168.7 (m, 4F_p), -169.1 (tt, 8F_m). $^{13}\text{C}\{^1\text{H}\}$ NMR (CD₃COCD₃, -90 °C, δ): 147.9 [dm, $^1J(\text{C-F}) = 225$ Hz, $^2J(\text{C-F}) = 24$ Hz, C-F_o, C₆F₅], 135.2 [dm, $^1J(\text{C-F}) = 250$ Hz, C-F_m, C₆F₅], 134.7 [dm, $^1J(\text{C-F}) \approx 230$ Hz, C-F_p, C₆F₅], 123.2 [s, $^2J(\text{C-Pt}) = 112$ Hz], 123.0 [s, $^2J(\text{C-Pt}) = 265$ Hz] (C_β, C_α≡C_βt-Bu), 80.8 [s, br, $^1J(\text{C-Pt}) = 843$ Hz, C_α, C_α≡C_βt-Bu], 57.7 (s, N-CH₂, NBu₄), 32.2 [s, C(CH₃)₃], 30.2 (s, CMe₃), 23.3, 19.6 [s, N-CH₂-(CH₂)₂-CH₃], 13.5 [s, N-(CH₂)₃-CH₃].

Synthesis of (NBu₄)₂[*cis*-Pt(C₆F₅)₂(μ-κC^α:η²-C≡CPh)₂]₂Cd], **3b**. [*cis*-Pt(C₆F₅)₂(t)ht]₂ (0.400 g, 0.567 mmol) was added to a fresh solution of LiC≡CPh (2.835 mmol) (1:5 molar ratio) in diethyl ether/hexane (20 mL) at low temperature (-40 °C). The mixture was warmed to room temperature, stirred for 30 min, and evaporated to dryness. The residue containing Li₂[*cis*-Pt(C₆F₅)₂(C≡CPh)₂] was treated with cold deoxygenated water (50 mL). The resulting colorless aqueous solution was filtered and added dropwise to an aqueous solution of (NBu₄)Br (0.457 g, 1.417 mmol), causing the formation of (NBu₄)₂[*cis*-Pt(C₆F₅)₂(C≡CPh)₂] as a white oily solid, which was washed with water (3 × 20 mL). The oil was dissolved in acetone (20 mL) and treated with a solution of Cd(NO₃)₂·4H₂O (0.087 g, 0.283 mmol) in water (~5 mL), precipitating immediately **3b** as a white solid. After 1 h of stirring, it is filtered, washed with water, and air-dried (0.355 g, 61% yield). Anal. Calcd for CdC₈₈H₉₂F₂₀N₂Pt₂ (2060.25): C, 51.30; H, 4.50; N, 1.36. Found: C, 51.60; H, 4.60; N, 1.27. Λ_M (acetonitrile): 217.2 Ω⁻¹·cm²·mol⁻¹. MALDI-TOF (-): *m/z* 1817 ([M + NBu₄]⁻ 19%), 695 ([Pt(C₆F₅)₃]⁻ 100%). IR (cm⁻¹): ν(C≡C) 2060s, 2031s; ν(C₆F₅)_{Xsens} 798 s, 792sh, 778s. ^1H NMR (CD₃COCD₃, 20 °C, δ): 7.74 (d, 8H, H_o, Ph), 7.20 (m, 12H, H_m+H_p, Ph), 3.47 (m, 16H, NCH₂, NBu₄), 1.85 (m, 16H, CH₂, NBu₄), 1.43 (m, 16H, CH₂, NBu₄), 0.98 (t, 24H, CH₃, NBu₄). ^{19}F NMR (CD₃COCD₃, 20 °C, δ): -115.1 [dm, $^3J(\text{Pt-F}_o) = 407$ Hz, 8F_o], -167.5 (m, 4F_p + 8F_m). $^{13}\text{C}\{^1\text{H}\}$ NMR (CD₃COCD₃, -90 °C, δ): 147.8 [dd, $^1J(\text{C-F}) = 224$ Hz, $^2J(\text{C-F}) = 24$ Hz, C-F_o, C₆F₅], 135.7 [dm, $^1J(\text{C-F}) \approx 245$ Hz, C-F_m/F_p, C₆F₅], 132.1 (s, C_o, Ph), 128.4 (s, C_m, Ph), 124.5 (s, C_i, Ph), 127.4 (s, C_p, Ph), 114.9 [s, $^2J(\text{C-Pt}) = 290$ Hz, C_β, C_α≡C_βPh], 92.6 [s, $^1J(\text{C-Pt}) = 844$ Hz, C_α, C_α≡C_βPh], 57.6 (s, N-CH₂, NBu₄), 23.2, 19.6 [s, N-CH₂-(CH₂)₂-CH₃], 13.6 [s, N-(CH₂)₃-CH₃].

Synthesis of (PMePh₃)₂[*cis*-Pt(C₆F₅)₂(μ-κC^α:η²-C≡CPh)₂]₂Cd], **3b'**. This complex was prepared similarly to complex **3a** starting from (PMePh₃)₂[*cis*-Pt(C₆F₅)₂(C≡CPh)₂] (0.125 g, 0.106 mmol) and Cd(NO₃)₂·4H₂O (0.016 g, 0.053 mmol), giving a white solid **3b'**, which was filtered off and washed with cold *i*-PrOH (0.070 g, 67% yield). Anal. Calcd for CdC₉₄F₂₀H₅₆P₂Pt₂ (2129.98): C, 53.01; H, 2.65. Found: C, 52.98; H, 2.99. Λ_M (acetone): 237.1 Ω⁻¹·cm²·mol⁻¹. MALDI-TOF (-): *m/z* 1852 ([M + NBu₄]⁻ 15%), 879 ([Pt(C≡CPh)₄(C₆F₅)₂Cd]⁻ 90%), 695 ([Pt(C₆F₅)₃]⁻ 100%). IR (cm⁻¹): ν(C≡C) 2060s, 2031s; ν(C₆F₅)_{Xsens} 798 s, 792sh, 778s. ^1H NMR (CD₃COCD₃, 20 °C, δ): 7.79 (m, 30H, Ph, PMePh₃ + 8H_o, C≡CPh), 7.14 (m, 12H, H_m+H_p, Ph), 3.14 [d, $^2J(\text{P-H}) = 14.0$ Hz, 6H, CH₃, PMePh₃]. ^{19}F NMR (CD₃COCD₃, 20 °C, δ): -115.1 [dm, $^3J(\text{Pt-F}_o) = 407$ Hz, 8F_o], -167.5 (m, 4F_p + 8F_m).

Synthesis of (NBu₄)₂[*cis*-Pt(C₆F₅)₂(μ-κC^α:η²-C≡CTol)₂]₂Cd], **3c**. Compound **3c** (white solid) was prepared following the same

Table 1. Crystal Data and Structure Refinement Details for **2c**·3(CH₃)₂CO, **3a**·H₂O, and **3b**

	2c ·3(CH ₃) ₂ CO	3a ·H ₂ O	3b
empirical formula	C ₇₇ H ₆₈ CdCl ₂ F ₁₀ O ₃ P ₂ Pt	C ₈₀ H ₁₀₈ CdF ₂₀ N ₂ OPt ₂	C ₈₈ H ₉₂ CdF ₂₀ N ₂ Pt ₂
fw	1671.64	1996.26	2060.22
temperature (K)	223(1)	173(1)	173(1)
wavelength (Å)	0.71073	0.71073	0.71073
cryst syst	monoclinic	orthorhombic	monoclinic
space group	C2/c	Pbca	Cc
a (Å); α (deg)	21.2846(3); 90	19.74250(10); 90	31.8250(3); 90
b (Å); β (deg)	18.2625(3); 98.3730(10)	24.69410(10); 90	17.0730(2); 126.6040(10)
c (Å); γ (deg)	19.0400(3); 90	38.1453(2); 90	19.2040(2); 90
V (Å ³); Z	7322.1(2); 4	18596.72(16); 8	8376.53(15); 4
calcd density (Mg/m ³)	1.516	1.426	1.634
abs corr (mm ⁻¹)	2.387	3.307	3.673
F(000)	3336	7952	4072
cryst size (mm ³)	0.40 × 0.40 × 0.15	0.30 × 0.30 × 0.20	0.1 × 0.1 × 0.1
2θ range (deg)	2.95 to 28.15	1.07 to 27.88	3.19 to 27.93
index ranges	0 ≤ h ≤ 27 0 ≤ k ≤ 24 −25 ≤ l ≤ 24	0 ≤ h ≤ 25 0 ≤ k ≤ 32 0 ≤ l ≤ 50	−41 ≤ h ≤ 41 −22 ≤ k ≤ 22 −21 ≤ l ≤ 25
no. refls collected	8788	22 077	64 994
no. of indep refls	8788 [R(int) = 0.0000]	22 077 [R(int) = 0.0000]	18 584 [R(int) = 0.0548]
no. of data/restraints/params	8788/0/440	22 077/1/825	18 584/2/835
goodness of fit on F ² ^a	1.481	1.069	1.162
final R indices [I > 2σ(I)] ^a	R1 = 0.0389, wR2 = 0.0827	R1 = 0.0588, wR2 = 0.1612	R1 = 0.0589, wR2 = 0.1367
R indices (all data) ^a	R1 = 0.0561, wR2 = 0.0900	R1 = 0.0908, wR2 = 0.1936	R1 = 0.0744, wR2 = 0.1437
largest diff peak and hole (e Å ⁻³)	1.065 and −1.143	2.163 and −2.341	1.806 and −2.416

^a $R_1 = \sum(|F_o| - |F_c|)/\sum|F_o|$; $wR_2 = [\sum w(F_o^2 - F_c^2)^2/\sum wF_o^2]^{1/2}$; goodness of fit = $[\sum[w(F_o^2 - F_c^2)^2]/(N_{\text{obs}} - N_{\text{param}})]^{1/2}$; $w = [\sigma^2(F_o^2) + (g_1P)^2 + g_2P]^{-1}$; $P = [\max(F_o^2; 0) + 2F_c^2]/3$.

procedure as for compound **3b**, but starting from [cis-Pt(C₆F₅)₂(thf)₂]⁷² (0.300 g, 0.446 mmol). The oil containing (NBu₄)₂[cis-Pt(C₆F₅)₂(C≡CTol)₂] was dissolved in acetone (20 mL) and treated with Cd(NO₃)₂·4H₂O (0.070 g, 0.223 mmol). After 1 h of stirring, the solution was evaporated to dryness and treated with *n*-hexane. The oily solid obtained was then treated with EtOH (5 mL) and stirred for 2 h, causing the precipitation of a white solid (0.188 g, 40% yield). Anal. Calcd for CdC₉₂F₂₀H₁₀₀N₂Pt₂ (2116.37): C, 52.21; H, 4.76; N, 1.32. Found: C, 51.98; H, 4.35; N, 1.28. Λ_M (acetonitrile): 212.7 Ω⁻¹·cm²·mol⁻¹. MALDI-TOF (−): *m/z* 1874 ([M + NBu₄]⁺ 34%), 695 ([Pt(C₆F₅)₃][−] 100%). IR (cm⁻¹): ν(C≡C) 2049m, 2024sh; ν(C₆F₅)_Xsens 790m, 784m. ¹H NMR (CD₃-COCD₃, 20 °C, δ): 7.63 (d, *J* = 7.8 Hz, 8H, C₆H₄, Tol), 6.99 (d, *J* = 7.7 Hz, 8H, C₆H₄, Tol), 3.43 (m, 16H, NCH₂, NBu₄), 2.24 (s, 12H, CH₃, Tol), 1.81 (m, 16H, CH₂, NBu₄), 0.97 (t, 24H, CH₃, NBu₄). ¹⁹F NMR (CD₃COCD₃, 20 °C, δ): −114.9 [dm, ³J(Pt–F_o) = 408 Hz, 8F_o], −167.7 (m, 4F_p + 8F_m). ¹³C{¹H} NMR (CD₃-COCD₃, −90 °C, δ): 147.8 [dd, ¹J(C–F) = 226 Hz, ²J(C–F) = 22 Hz, C–F_o, C₆F₅], 135.5 [dm, ¹J(C–F) ≈ 235 Hz, C–F_m/F_p, C₆F₅], 136.9 (s, C⁴, Tol), 132.2 (s, CH, Tol), 129.1 (s, CH, Tol), 121.6 (s, C¹, Tol), 114.2 [s, br ²J(C–Pt) = 282 Hz, C_β, C_α≡C_βPh], 92.2 [s, ¹J(C–Pt) = 851 Hz, C_α, C_α≡C_βTol], 57.7 (s, N–CH₂, NBu₄), 23.3, 19.6 [s, N–CH₂–(CH₂)₂–CH₃], 20.9 (s, CH₃, Tol), 13.6 [s, N–(CH₂)₃–CH₃].

Synthesis of (PMePh₃)₂[{cis-Pt(C₆F₅)₂(μ-κC^α:η²-C≡CTol)₂]₂-Cd], **3c'.** Compound **3c'** (white solid) was prepared following the same procedure as for compound **3a**, but starting from (PMePh₃)₂[cis-Pt(C₆F₅)₂(C≡CTol)₂] (0.150 g, 0.114 mmol) and Cd(NO₃)₂·4H₂O (0.018 g, 0.057 mmol) (0.113 g, 91% yield). Anal. Calcd for CdC₉₈F₂₀H₆₄P₂Pt₂ (2186.09): C, 53.84; H, 2.95. Found: C, 53.67; H, 2.92%. Λ_M (acetone): 237 Ω⁻¹·cm²·mol⁻¹. MALDI-TOF (−): *m/z* 1909 ([M + PMePh₃]⁺ 9%), 1632 ([M]⁺ 10%), 695 ([Pt(C₆F₅)₃][−] 100%). IR (cm⁻¹): ν(C≡C) 2049m, 2024sh; ν(C₆F₅)_Xsens 790m, 784m. ¹H NMR (CD₃COCD₃, 20 °C, δ): 7.86 (m, 30H, Ph, PMePh₃), 7.63 (d, *J* = 7.6 Hz, 8H, C₆H₄, Tol), 6.99 (d, *J* = 7.6 Hz, 8H, C₆H₄, Tol), 3.16 [d, ²J(P–H) = 14.0 Hz, 6H, CH₃, PMePh₃], 2.21 (s, 12H, CH₃, Tol). ¹⁹F NMR (CD₃COCD₃, 20 °C, δ): −114.9 [dm, ³J(Pt–F_o) = 408 Hz, 8F_o], −167.5 (m, 4F_p + 8F_m).

(72) Usón, R.; Forniés, J.; Tomás, M.; Menjón, B. *Organometallics* **1985**, *4*, 1912.

X-ray Crystallography. Table 1 reports details of the structural analyses for the complexes **2c**·3Me₂CO, **3a**·H₂O, and **3b**. Colorless crystals were obtained by slow diffusion of hexane into an acetone (**2c**), ethanol (**3a**), or dichloromethane (**3b**) solution of each compound at −30 °C. For complex **2c**, 1.5 molecules of acetone were found in the asymmetric unit. Complex **3a** crystallizes with a water molecule. X-ray intensity data were collected with a NONIUS κCCD area-detector diffractometer, using graphite-monochromated Mo Kα radiation (λ(Mo Kα) 0.71071 Å). Images were processed using the DENZO and SCALEPACK suite of programs,⁷³ carrying out the absorption correction at this point for complexes **2c**·3Me₂CO and **3a**·H₂O, and for complex **3b** the absorption correction was performed using SORTAV.⁷⁴ The structures were solved by direct methods using the SHELXS-97 program⁷⁵ and refined by full-matrix least squares on F² with SHELXL-97.⁷⁶ All non-hydrogen atoms were assigned anisotropic displacement parameters. The hydrogen atoms were constrained to idealized geometries fixing isotropic displacement parameters of 1.2 times the U_{iso} value of their attached carbons for phenyl and methylene hydrogens and 1.5 for the methyl groups. For complexes **3a**·H₂O and **3b** residual peaks larger than 1 e Å⁻³ have been observed but with no chemical significance, and a common set of thermal anisotropic parameters were used for some atoms.

Results and Discussion

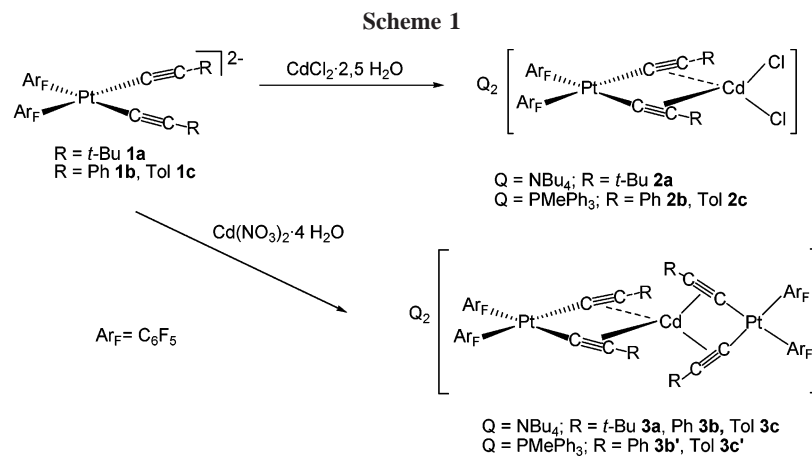
Synthesis and Characterization. Treatment of Q₂[cis-Pt(C₆F₅)₂(C≡CR)₂] (Q = NBu₄, R = *t*-Bu **1a**; Q = PMePh₃, R = Ph **1b**, R = Tol **1c**) with 1 equiv of CdCl₂·2.5H₂O in acetone afforded the colorless binuclear 1:1 adducts Q₂[{cis-Pt(C₆F₅)₂(μ-κC^α:η²-C≡CR)₂]₂(CdCl₂)] **2a–2c** in moderate to high yields (55–77%) (Scheme 1). By contrast, the reaction of (NBu₄)₂[cis-Pt(C₆F₅)₂(C≡CR)₂], for R = Ph and Tol prepared in situ

(73) Otwinowski, Z.; Minor, W. In *Methods in Enzymology*; Carter, C. V., Jr., Sweet, R. M., Eds.; Academic Press: New York, 1997; Vol. 276A, p 307.

(74) Blessing, R. H. *Acta Crystallogr.* **1995**, *A51*, 33.

(75) Sheldrick, G. M. *SHELXS97, a Program for the Solution of Crystal Structures*; University of Göttingen: Göttingen, Germany, 1997.

(76) Sheldrick, G. M. *SHELXL97, a Program for the Refinement of Crystal Structures*; University of Göttingen: Germany, 1997.



as oily products, with $\text{Cd}(\text{NO}_3)_2 \cdot 4\text{H}_2\text{O}$ in 1:1 or 2:1 molar ratio gave the trinuclear dianionic complexes $(\text{NBu}_4)_2[\{\text{cis-Pt}(\text{C}_6\text{F}_5)_2(\mu\text{-}\kappa\text{C}^\alpha\text{:}\eta^2\text{-C}\equiv\text{CR})_2\}_2\text{Cd}]$ ($\text{R} = t\text{-Bu } \mathbf{3a}$, $\text{Ph } \mathbf{3b}$, $\text{Tol } \mathbf{3c}$), respectively. The analogous $(\text{PMePh}_3)_2[\{\text{cis-Pt}(\text{C}_6\text{F}_5)_2(\mu\text{-}\kappa\text{C}^\alpha\text{:}\eta^2\text{-C}\equiv\text{CR})_2\}_2\text{Cd}]$ ($\text{R} = \text{Ph } \mathbf{3b'}$, $\text{Tol } \mathbf{3c'}$) were prepared similarly starting from $(\text{PMePh}_3)_2[\text{cis-Pt}(\text{C}_6\text{F}_5)_2(\text{C}\equiv\text{CR})_2]$; see Experimental Section for details. All complexes have been characterized by the usual analytical and spectroscopic techniques, and, in the case of complexes $\mathbf{2c}$ and $\mathbf{3a,b}$, their structures were confirmed by X-ray crystallography. Interestingly, in all trinuclear derivatives ($\mathbf{3}$), the peak corresponding to $[\text{Pt}_2(\text{C}_6\text{F}_5)_4(\text{C}\equiv\text{CR})_4\text{Cd} + \text{Q}]^-$ is seen in the mass spectra using the MALDI-TOF technique. The most relevant spectroscopic feature appears in the IR spectra, which shows one ($\mathbf{3a}$) or two ($\mathbf{2a}$, $\mathbf{2c}$, $\mathbf{3c}$ one as a shoulder) $\nu(\text{C}\equiv\text{C})$ stretching vibrations ($2022\text{--}2060 \text{ cm}^{-1}$), as expected, shifted to lower wavenumbers compared to the corresponding ones in the precursors $\text{Q}_2[\text{cis-Pt}(\text{C}_6\text{F}_5)_2(\text{C}\equiv\text{CR})_2]$ ($\text{Q} = \text{NBu}_4$, $\text{R} = t\text{-Bu } 2090, 2085 \text{ cm}^{-1}$; $\text{Q} = \text{PMePh}_3$, $\text{R} = \text{Ph } 2096, 2083 \text{ cm}^{-1}$; $\text{R} = \text{Tol } 2091, 2078 \text{ cm}^{-1}$). Bimetallic complexes $\mathbf{2}$ are not soluble enough to register $^{13}\text{C}\{^1\text{H}\}$ NMR spectra. However, in the case of trinuclear complexes $\mathbf{3a-c}$, the $^{13}\text{C}\{^1\text{H}\}$ NMR spectra at low temperature ($-90 \text{ }^\circ\text{C}$) in CD_3COCD_3 reveal that upon η^2 -coordination of the alkyne ligands to a Cd^{2+} center, the signals due to the C_α and C_β atoms of the $\text{Pt-C}\equiv\text{C}$ entities shift upfield for C_α and downfield for C_β [i.e., δ 92.2 (C_α), 114.2 (C_β) $\mathbf{3c}$ vs 117.3 (C_α), 103.7 (C_β) $\mathbf{1c}$]. This result is in agreement with previous observations made by us in related systems in which the terminal alkynyl ligand is η^2 -coordinated to a second metal center.^{77–79} The assignment of both signals is based on the observed coupling to ^{195}Pt nuclei [δ $\text{C}_\alpha/{}^1J(\text{C-Pt})$ 80.8/843 Hz $\mathbf{3a}$; 92.6/844 Hz $\mathbf{3b}$; 92.2/851 Hz $\mathbf{3c}$ and $\text{C}_\beta/{}^2J(\text{C-Pt})$ 114.9/290 Hz $\mathbf{3b}$; 114.2/282 Hz $\mathbf{3c}$]. In the case of complex $\mathbf{3a}$, two close C_β signals (123.2; 123.0) flanked by two different sets of Pt satellites (112 Hz, 265 Hz) are resolved, although in the proton spectrum at low temperature ($-90 \text{ }^\circ\text{C}$) only one $t\text{-Bu}$ resonance is observed. We noted that both the ${}^1J(\text{C}_\alpha\text{-Pt})$ and ${}^2J(\text{C}_\beta\text{-Pt})$ platinum coupling constants are notably smaller in these Pt_2Cd complexes than those observed in the precursors (i.e., 851 and 282 Hz in $\mathbf{3c}$ vs 1075, 308 Hz in $\mathbf{1c}$), reflecting^{77–79} the expected lower degree of s orbital participation in the platinum–carbon alkynyl bridging bond due to a partial rehybridization of the carbon atoms toward sp^2 .

(77) Ara, I.; Berenguer, J. R.; Forniés, J.; Lalinde, E. *Organometallics* **1997**, *16*, 3921.

(78) Berenguer, J. R.; Forniés, J.; Lalinde, E.; Martínez, F. *Organometallics* **1996**, *15*, 4537.

(79) Ara, I.; Berenguer, J. R.; Eguizábal, E.; Forniés, J.; Lalinde, E.; Martín, A.; Martínez, F. *Organometallics* **1998**, *17*, 4578.

X-ray structural determinations of $\mathbf{2c}$, $\mathbf{3a}$, and $\mathbf{3b}$ have been performed (Figures 1, 2, and 3), and selected bond lengths and angles are listed in Table 2. $\mathbf{2c}$ crystallizes in the monoclinic space group $C2/c$ with four independent molecules per unit cell. Its molecular structure confirms that the heterobimetallic anion is formed by the dianionic fragment $\{\text{cis-Pt}(\text{C}_6\text{F}_5)_2(\text{C}\equiv\text{CR})_2\}^{2-}$ acting as a bis(η^2 -alkyne)chelate ligand toward the CdCl_2 unit. The two chlorine atoms complete a distorted tetrahedral coordination for the cadmium atom ($74.27(17)^\circ$ for $\text{C}(1)\text{---Cd---C}(1a)$ to $120.25(5)^\circ$ for $\text{Cl}(1)\text{---Cd---Cl}(1a)$) with Cd---Cl bond lengths (2.4250(10) Å) very similar to those observed in $[\{\text{Pt}(\text{C}\equiv\text{CPh})_4\}(\text{CdCl}_2)_2]^{2-}$.⁶⁸ The Cl---Cd---Cl fragment lies almost perpendicular to the coordination plane of the platinum atom (89.46°). Both $\text{C}\equiv\text{CR}$ units are asymmetrically η^2 -coordinated to Cd, showing Cd---C_α bond lengths [2.405(3) Å]

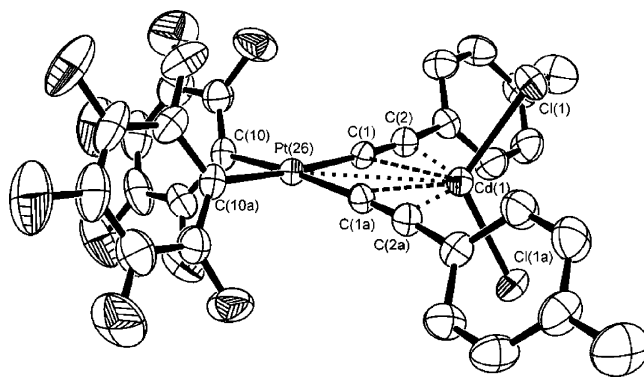


Figure 1. Molecular structure of the anion $[\{\text{cis-Pt}(\text{C}_6\text{F}_5)_2(\mu\text{-}\kappa\text{C}^\alpha\text{:}\eta^2\text{-C}\equiv\text{CTol})_2\}(\text{CdCl}_2)_2]^{2-}$ in $\mathbf{2c}$. Ellipsoids are drawn at the 50% probability level. Hydrogen atoms are omitted for clarity.

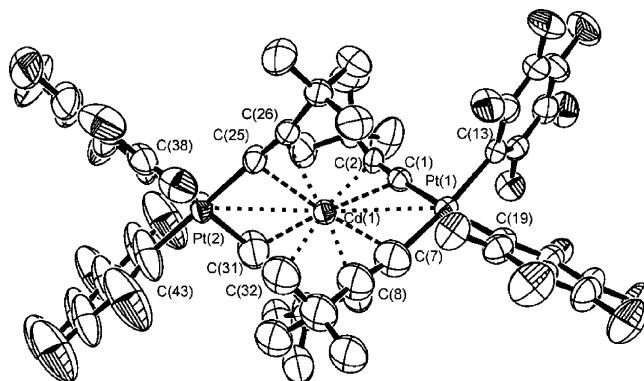


Figure 2. Molecular structure of the anion $[\{\text{cis-Pt}(\text{C}_6\text{F}_5)_2(\mu\text{-}\kappa\text{C}^\alpha\text{:}\eta^2\text{-C}\equiv\text{C}t\text{-Bu})_2\}_2\text{Cd}]^{2-}$ in $\mathbf{3a}$. Ellipsoids are drawn at the 50% probability level. Hydrogen atoms are omitted for clarity.

Table 2. Selected Bond Lengths [Å] and Angles [deg] for Complexes (PMePhes)₂[{*cis*-Pt(C₆F₅)₂(μ-κC^α:η²-C≡CTol)₂}(CdCl₂)]·3(CH₃)₂CO, 2c·3(CH₃)₂CO, (NBu₄)₂[{*cis*-Pt(C₆F₅)₂(μ-κC^α:η²-C≡Ct-Bu)₂}(Cd)]·H₂O, 3a·H₂O, and (NBu₄)₂[{*cis*-Pt(C₆F₅)₂(μ-κC^α:η²-C≡CPh)₂}(Cd)], 3b

		Complex 2c·3(CH ₃) ₂ CO			
Pt(1)–Cd(1)	3.2998(4)	Cd(1)–Cl(1)	2.4250(10)	C(1)–C(2)	1.222(5)
Cd(1)–C(1)	2.405(3)	Cd(1)–C(2)	2.556(4)		
C(1)–Pt(1)–C(1a)	92.78(19)	C(2)–C(1)–Pt(1)	176.3(3)	C(1)–C(2)–C(3)	173.7(4)
Cl(1)–Cd(1)–Cl(1)	120.25(5)				
		Complex 3a·H ₂ O			
Pt(1)–Cd(1)	3.1748(5)	Cd(1)–C(8)	2.589(11)	C(1)–C(2)	1.233(9)
Pt(2)–Cd(1)	3.2063(5)	Cd(1)–C(25)	2.377(7)	C(7)–C(8)	1.241(14)
Cd(1)–C(1)	2.365(7)	Cd(1)–C(26)	2.591(7)	C(25)–C(26)	1.203(10)
Cd(1)–C(2)	2.657(7)	Cd(1)–C(31)	2.374(11)	C(31)–C(32)	1.190(14)
Cd(1)–C(7)	2.407(12)	Cd(1)–C(32)	2.610(11)		
C(7)–Pt(1)–C(1)	95.1(4)	C(1)–C(2)–C(3)	168.4(7)	C(25)–C(26)–C(27)	167.3(7)
C(25)–Pt(2)–C(31)	94.5(4)	C(8)–C(7)–Pt(1)	167.1(12)	C(32)–C(31)–Pt(2)	177.9(14)
Pt(1)–Cd(1)–Pt(2)	169.523(19)	C(7)–C(8)–C(9)	167.9(13)	C(31)–C(32)–C(33)	167.7(12)
C(2)–C(1)–Pt(1)	176.9(6)	C(26)–C(25)–Pt(2)	175.7(7)		
		Complex 3b			
Pt(1)–Cd(1)	3.2173(12)	Cd(1)–C(10)	2.547(12)	C(1)–C(2)	1.151(17)
Pt(2)–Cd(1)	3.2863(12)	Cd(1)–C(29)	2.376(12)	C(9)–C(10)	1.197(17)
Cd(1)–C(1)	2.387(10)	Cd(1)–C(30)	2.561(12)	C(29)–C(30)	1.243(16)
Cd(1)–C(2)	2.528(12)	Cd(1)–C(37)	2.418(10)	C(37)–C(38)	1.209(16)
Cd(1)–C(9)	2.385(11)	Cd(1)–C(38)	2.552(11)		
C(29)–Pt(2)–C(37)	91.7(4)	C(1)–C(2)–C(3)	171.7(12)	C(29)–C(30)–C(31)	169.7(13)
C(9)–Pt(1)–C(1)	92.8(4)	C(10)–C(9)–Pt(1)	176.6(11)	C(38)–C(37)–Pt(2)	176.9(10)
Pt(1)–Cd(1)–Pt(2)	174.37(4)	C(9)–C(10)–C(11)	166.9(13)	C(37)–C(38)–C(39)	170.1(12)
C(2)–C(1)–Pt(1)	175.4(12)	C(30)–C(29)–Pt(2)	177.3(11)		

that are slightly shorter than the corresponding Cd–C_β [2.556–(4) Å] ones. This type of asymmetry has been also previously found in the trinuclear anion [{Pt(C≡CPh)₄}(CdCl₂)₂]²⁻. However, in contrast to this anion, which exhibits nonplanar PtC₄–Cd cores, given that the Cd atoms are displaced from the Pt(II) coordination plane, in [{*cis*-Pt(C₆F₅)₂(C≡CTol)₂}(CdCl₂)²⁻ (**2c**), the Cd is almost in *plane*-bound with Pt(1), C(1), C(1a), C(10), C(10a) (max. deviation from this plane, C(1) 0.0348 Å) leading to a flat PtC₄Cd core. The preference for *in-plane* bis(η²-alkyne) bonding interactions has been found to be a typical characteristic of early–late [Ti](C≡CR)₂ML_n ([Ti] = Cp₂Ti, (η⁵-C₅H₄SiMe₃)₂-Ti, M = d¹⁰ metal fragment),^{8,53,55} while [{*cis*-Pt(C≡CR)₂ML_n}] tweezer systems usually exhibit hinged structures.^{5,8,53,77,78,80–83} However, this structural feature is not unprecedented in platinum chemistry, having been previously observed in the heterobimetallic anions [{*cis*-Pt(C₆F₅)₂(C≡CSiMe₃)₂}(MX₂)²⁻ (MX₂ = HgBr₂,⁶² CoCl₂)⁸⁴], which also show planar PtC₄M cores. The Pt–Cd distance [3.2998(4) Å], although close to the sum of the van der Waals radii (3.3 Å), is clearly out of the range [2.639(1)–2.960(1) Å] observed in complexes having donor→acceptor Pt→Cd bonds (i.e., [(Phy)₂Pt-

(cyclen)]²⁺ 2.639(1) Å,⁸⁵ [(bzq)(C₆F₅)₂PtCd(cyclen)] 2.688(1) Å,⁶⁷ suggesting that only a weak interaction, if any, is present. It should be noted that despite the η²-coordination of both C≡CTol units to Cd(1), the alkynyl entities deviate only slightly from linearity, this effect being more important at C_β [173.7–(4)°] than at C_α [176.3(3)°] carbon atom.

The molecular structures of the anions **3a** and **3b** confirm that they are new examples of very rare bis(tweezer) type complexes constructed from two dianionic fragments {*cis*-Pt(C₆F₅)₂(C≡CR)₂}²⁻ connected by a naked Cd²⁺ ion. To the best of our knowledge, only a few examples of trinuclear cationic complexes Pt₂Ag, Pt₂Cu, and Ti₂Ag formed by two orthogonal neutral L_nM(C≡CR)₂ fragments acting as bidentate diyne ligands toward Cu(I) or Ag(I) have been previously reported.^{8,86–89} In both anions, the two platinum coordination planes are oriented almost perpendicularly to each other, the dihedral angle C_α–Pt(1)–C_α/C_α–Pt(2)–C_α being 84.16° for **3a** and 82.71° for **3b**. The Cd atom is embedded within the alkynyl fragments and is tetrahedrally coordinated by four alkyne units. These complexes represent the first reported examples in which a Cd(II) ion is stabilized only by η²-alkyne bonding interactions. In both anions, the Cd–alkynide η²-linkages are asymmetric, the Cd–C_α bond distances [2.365(7)–2.407(12) Å **3a**, 2.376(12)–2.418(10) Å **3b**]

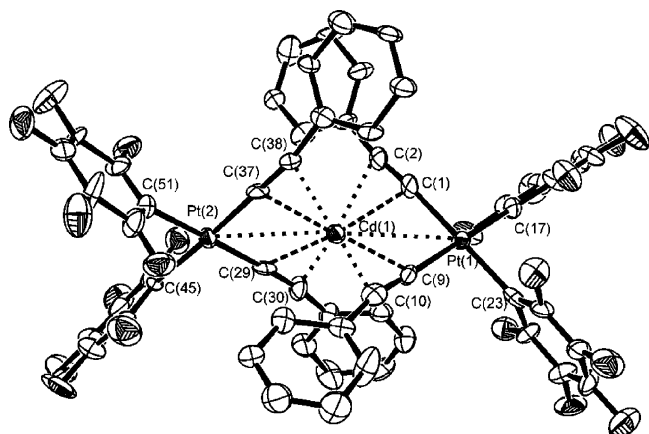


Figure 3. Molecular structure of the anion [{*cis*-Pt(C₆F₅)₂(μ-κC^α:η²-C≡CPh)₂}(Cd)]²⁻ in **3b**. Ellipsoids are drawn at the 50% probability level. Hydrogen atoms are omitted for clarity.

(80) Ara, I.; Falvello, L. R.; Fernández, S.; Forniés, J.; Lalinde, E.; Martín, A.; Moreno, M. T. *Organometallics* **1997**, *16*, 5923.

(81) Ara, I.; Berenguer, J. R.; Eguizábal, E.; Forniés, J.; Lalinde, E.; Martínez, F. *Organometallics* **1999**, *18*, 4344.

(82) Berenguer, J. R.; Eguizábal, E.; Falvello, L. R.; Forniés, J.; Lalinde, E.; Martín, A. *Organometallics* **2000**, *19*, 490.

(83) Ara, I.; Berenguer, J. R.; Eguizábal, E.; Forniés, J.; Lalinde, E. *Organometallics* **2001**, *20*, 2686.

(84) Ara, I.; Berenguer, J. R.; Forniés, J.; Lalinde, E. *Inorg. Chim. Acta* **1997**, *264*, 199.

(85) Yamaguchi, T.; Yamazaki, F.; Ito, T. *J. Am. Chem. Soc.* **1999**, *121*, 7405.

(86) Ara, I.; Berenguer, J. R.; Forniés, J.; Lalinde, E.; Moreno, M. T. *J. Organomet. Chem.* **1996**, *50*, 63.

(87) Yamazaki, S.; Deeming, A. J. *J. Chem. Soc., Dalton Trans.* **1993**, 3051.

(88) Yamazaki, S.; Deeming, A. J.; Hursthouse, M. B.; Malik, K. M. A. *Inorg. Chim. Acta* **1995**, *235*, 147.

(89) Hayashi, Y.; Osawa, M.; Kobayashi, K.; Sato, T.; Sato, M.; Wakatsuki, Y. *J. Organomet. Chem.* **1998**, *569*, 169.

Table 3. Absorption Data ($\sim 5 \times 10^{-5}$ M CH_2Cl_2 Solutions)

	absorption [nm] ($10^3 \epsilon/\text{M}^{-1} \text{cm}^{-1}$)
1a	220sh (10.4), 231 (17.5), 243sh (14.8), 295sh (5.8)
1b	232 (42.8), 275 (22.6), 290 (21.8), 310 (19.4), 325sh (12.4) ^a
1c	219sh (13.0), 232 (35.6), 268 (16.9), 275 (17.0), 293 (15.2), 311 (13.4), 331sh (7.2)
2a	219sh (9.4), 232 (17.6), 240sh (15.0), 277sh (8.5)
2b	220sh (16.2), 234 (50.2), 262 (31.8), 268 (33.3), 275 (31.5), 309 (21.6)
2c	219sh (11.7), 231 (31.3), 262 (16.4), 268 (17.5), 274 (16.7), 308 (11.4)
3a	220sh (17.0), 233 (37.3), 278sh (16.6)
3b	220sh (17.4), 233 (41.6), 263 (39.7), 307sh (22.3)
3b'	217sh (15.9), 234 (55.6), 262 (43.0), 267 (43.2), 275 (39.6), 308sh (22.2)
3c	219sh (20.0), 235 (40.5), 268 (48.0), 308sh (26.0)
3c'	216sh (19.8), 231 (45.8), 262 (22.7), 267 (23.0), 274sh (20.7), 309 (13.0)

^a See ref 67.

being shorter than the corresponding Cd–C β [2.589(11)–2.657(7) Å **3a**; 2.528(12)–2.561(12) Å **3b**] ones. This structural feature has also been found in the related trinuclear cations [Pt(PPh₃)₂(C≡CPh)₂Ag]⁺,⁸⁶ [PtL₂(C≡CPh)₂Cu]⁺,⁸⁷ (L = dppe, bipy), and [TiCp'2(C≡CR)₂Ag]⁺ (Cp' = C₅H₄SiMe₃, R = Ph, Fc)⁸⁹ and in the heteropentanuclear AgAu₄ cation [Ag–{(AuL)₂{μ-Ar(C≡CR)₂}₂}₂]⁺ (Ar = C₆Me₄), respectively. The Cd–C(alkynyl) distances, which are comparable to those found in **2c**, are more asymmetric in the *tert*-butyl derivative **3a** than in the phenylethynyl anion **3b**, this being reflected in the distortion of the alkynyl ligands (167.1(12)–177.9(14)° at C α and 167.3(7)–168.4(7)° at C β in **3a** vs 175.4(12)–177.3(11) at C α and 166.9(13)–171.7(12) at C β in **3b**). The Pt–Cd–Pt entity is almost linear [169.523(19)° in **3a** vs 174.37(4)° in **3b**] and the Pt–Cd distances [3.1748(5), 3.2063(5) Å **3a**; 3.2863(12), 3.2173(12) Å **3b**] are slightly shorter than in **2c** [3.2998(4) Å].

Electronic and Luminescence Spectroscopy. Absorption spectra for complexes **2** and **3** and their heteroleptic bis-(pentafluorophenyl)bis(alkynyl)platinate(II) precursors, **1**, were obtained in CH₂Cl₂, and the results are shown in Table 3. The absorption spectra of the precursors Q₂[*cis*-Pt(C₆F₅)₂(C≡CR)₂] **1a**–**1c** display a very intense high-energy (~ 231 – 232 nm) and a broad absorption profile with several maxima at lower energies (~ 260 – 295 nm **1a**; 275–325 nm **1b**; 268–331 nm **1c**). The high-energy band (~ 231 – 232 nm), which occurs at a similar energy to that seen in (NBu₄)₂[Pt(C₆F₅)₄] (236, 290sh), is mainly attributed to $\pi\pi^*$ transitions in C₆F₅ groups, though a presumable overlapping with bands, due to the cation PMePh₃⁺, in complexes **1b** and **1c** is to be expected. The broad absorption profile located in the near-UV region is ascribed to the C≡CR alkynyl ligands. With reference to previous spectroscopic works,^{26,28,34,40,47,50,91–94} and in agreement with theoretical calculations⁹⁵ in alkynyl platinum complexes,^{91,94,96–98} the lowest

(90) Vicente, J.; Chicote, M. T.; Alvarez-Falcón, M. M.; Jones, P. G. *Organometallics* **2005**, *24*, 4666.

(91) Benito, J.; Berenguer, J. R.; Forniés, J.; Gil, B.; Gómez, J.; Lalinde, E. *Dalton Trans.* **2003**, 4331.

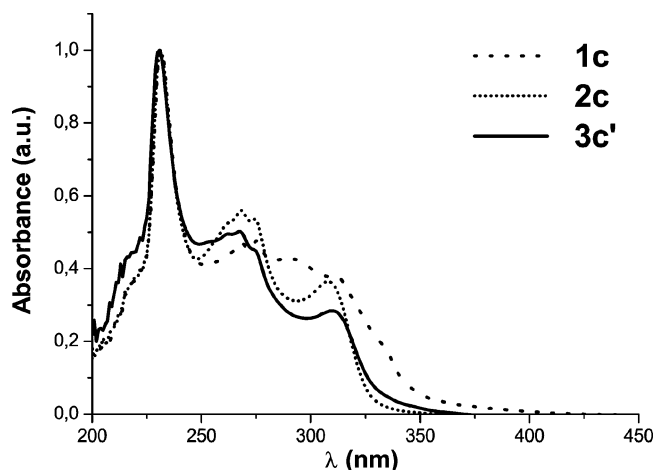
(92) Kwok, W. M.; Phillips, D. L.; Yeung, P. K. Y.; Yam, V. W. W. *J. Phys. Chem. A* **1997**, *101*, 9286.

(93) Haskins-Glusac, K.; Chiriuga, I.; Abboud, K. A.; Schanze, K. S. *J. Phys. Chem. B* **2004**, *108*, 4969.

(94) Emmert, L. A.; Choi, W.; Marshall, J. A.; Yang, J.; Meyer, L. A.; Brozik, J. A. *J. Phys. Chem. A* **2003**, *107*, 11340.

(95) Theoretical calculations in alkynyl platinum complexes have shown that the HOMO is mainly dominated by the antibonding character of the Pt–C≡CR moiety resulting from the overlap of the d π (Pt) and π (C≡CR) orbitals, while the LUMO has little electron density located on the platinum metal and has a predominantly π^* (C≡CR) character.

(96) Yip, H. K.; Lin, H. M.; Wang, Y.; Che, C. M. *J. Chem. Soc., Dalton Trans.* **1993**, 2939.

**Figure 4.** Absorption spectra of tolylalkynyl derivatives **1c**, **2c**, and **3c'** in CH₂Cl₂ ($\sim 5 \times 10^{-5}$ M).

energy band, in each case, can be assigned to an admixture of $\pi \rightarrow \pi^*$ (C≡CR) IL/d π (Pt) $\rightarrow \pi^*$ (C≡CR) MLCT but with a predominant intraligand character. The low-energy absorption in the spectra of **1b** (~ 325 nm) and **1c** (~ 330 nm) in CH₂Cl₂ is blue-shifted when compared to the homoleptic complexes Q₂[Pt(C≡CR)₄] (R = Ph, 347; R = Tol, 345 nm),⁹¹ probably due to the presence of the C₆F₅ ligands, which presumably somewhat stabilize the energy of the d π platinum orbitals, increasing the energy of the corresponding ¹MLCT. In contrast to the electron-releasing nature of the “Pt(C₆F₅)₂” fragment, recent electrochemical and theoretical calculations^{97–101} indicate that the alkynyl group acts mainly as a σ/π donor with essentially no back-donation from the metal, and therefore, the “Pt(C≡CR)₂” fragment is more electron rich.

The absorption spectra of complexes **2** (PtCd) and **3** (Pt₂Cd) with the same counterion are quite similar (see Table 3). By way of illustration, the spectra of complexes with tolylalkynyl ligands **1c**, **2c**, and **3c'** are shown in Figure 4. In the arylalkynyl derivatives, the high-energy bands at 231–235 and 262–275 nm, respectively, appear at similar energies in relation to the mononuclear precursors, being similarly attributed to ligand-centered transitions (¹LC, $\pi\pi^*$ C₆F₅ and C≡C-aryl). The most significant difference in these bi- and trimetallic complexes is found in the low-energy absorption, which exhibits a clear hypsochromic shift and λ_{max} decreases compared to their respective precursors. The blue-shift of the low IL $\pi\pi^*$ (C≡CR)/MLCT absorption in complexes **2** (PtCd) and **3** (Pt₂Cd) can be rationalized by the existence of a lesser bonding interaction between the Pt center (d π orbitals) and the C≡CR fragment upon η^2 -complexation to CdCl₂ (**2**) or Cd²⁺ (**3**), which decreases the extent of π -conjugation, causing an increase of the band gap. In addition, it is also evident from Figure 4 (for **1c**) that in the mononuclear complexes **1b** and **1c** the 275–350 nm region is broader and somewhat more complex than in the polymeric complexes **2** and **3**. This could be attributed to the fact that the *in-plane* η^2 -complexation presumably constrains the rotation around the alkynyl–chain axis, leading to less heterogeneity with respect to conjugation along the C≡C-aryl ligand and between both alkynyl groups via the Pt center.

(97) Zhuravlev, F.; Gladysz, J. A. *Chem. Eur. J.* **2004**, *10*, 6510.

(98) Springborg, M.; Albers, R. C. *Phys. Rev. B* **1996**, *53*, 10626.

(99) Wong, C. Y.; Che, C. M.; Chan, M. C. W.; Han, J.; Leung, K. H.; Phillips, D. L.; Wong, K. Y.; Zhu, N. *J. Am. Chem. Soc.* **2005**, *127*, 13997.

(100) Jones, S. C.; Coropceanu, V.; Barlow, S.; Kinnibrugh, T.; Brédas, J. L.; Marder, S. R. *J. Am. Chem. Soc.* **2004**, *126*, 11782.

(101) Louwen, J. N.; Hengelmolen, R.; Grove, D. M.; Oskam, A.; Dekock, R. L. *Organometallics* **1984**, *3*, 908.

Table 4. Photophysical Data for Complexes

compound ^a	medium	λ_{em} [nm]	τ [μs]
1b^b	solid (298 K)	451 ^c (λ_{ex} 350)	7.4 (λ_{em} 450)
	solid (77 K)	444 _{max} , 464, 475, 489, 515 ^c (λ_{ex} 330–360)	48.3 (λ_{em} 445)
1c	CH ₂ Cl ₂ 10 ⁻³ M (77 K)	430 _{max} , 452, 471 ^c (λ_{ex} 320)	8.0 (λ_{em} 454);
	solid (298 K)	454 _{min} , 531 _{max} (λ_{ex} 360)	8.0 (30%), 53.2 (70%) (λ_{em} 540)
2a^d	solid (77 K)	545 (λ_{ex} 390)	42.6 (λ_{em} 450)
	solid (77 K)	451 _{max} , 472 ^c (λ_{ex} 360)	15.4 (60%), 42.6 (40%) (λ_{em} 450);
2a^d	CH ₂ Cl ₂ 10 ⁻³ M (298 K)	427 (λ_{ex} 370)	15.4 (52%), 92.3 (48%) (λ_{em} 530)
	CH ₂ Cl ₂ 10 ⁻³ M (77 K)	429, 474 _{max} , 523sh ^c (λ_{ex} 320)	
2a^d	solid (77 K)	429 _{min} , 523 _{max} , 558sh ^c (λ_{ex} 380)	64.2 (λ_{em} 426)
	solid (77 K)	426 _{max} , 463 ^c (λ_{ex} 305)	
2a^d	solid (77 K)	463 _{max} , 495 ^c (λ_{ex} 340)	12.4 (73%), 117.3 (27%) (λ_{em} 495)
	solid (77 K)	463 _{min} , 495 _{max} , 530 ^c (λ_{ex} 370)	
2a^d	CH ₂ Cl ₂ 10 ⁻³ M (77 K)	427, 450, 480, 515 (λ_{ex} 305)	
	solid (77 K)	450, 480, 515 (λ_{ex} 360)	
2b	solid (298 K)	480 _{max} , 515, 555 (λ_{ex} 390)	23.0 (λ_{em} 425)
	solid (77 K)	425, 444, 460 _{max} , 482sh (λ_{ex} 360)	28.4 (λ_{em} 420)
2b	CH ₂ Cl ₂ 10 ⁻³ M (298 K)	421 _{max} , 440, 450, 460 ^c (λ_{ex} 360)	
	CH ₂ Cl ₂ 10 ⁻³ M (77 K)	400 ^d (λ_{ex} 340)	
2c	CH ₂ Cl ₂ 10 ⁻³ M (77 K)	423 _{max} , 443, 453, 470 ^c (λ_{ex} 340)	23.6 (λ_{em} 430)
	solid (298 K)	430, 451 _{max} , 490sh ^c (λ_{ex} 320)	121 (λ_{em} 490)
2c	solid (77 K)	430 _{min} , 451, 490 _{max} , 520sh ^c (λ_{ex} 360)	77.5 (λ_{em} 428)
	solid (77 K)	420, 425, 445 _{max} , 470sh ^c (λ_{ex} 300)	39.7 (81%), 155.6 (19%) (λ_{em} 470)
2c	CH ₂ Cl ₂ 10 ⁻³ M (298 K)	420 _{min} , 449 _{max} , 470 ^c (λ_{ex} 330)	
	CH ₂ Cl ₂ 10 ⁻³ M (77 K)	406, 417sh, 493 _{min} (λ_{ex} 300–340)	
3a^d	CH ₂ Cl ₂ 10 ⁻³ M (77 K)	426 _{max} , 450, 468, 486sh (λ_{ex} 320)	72.4 (λ_{em} 430); 12.4 (λ_{em} 447)
	solid (77 K)	426 _{min} , 457, 486 _{max} , 516sh ^c (λ_{ex} 350)	
3b	solid (77 K)	430, 447 (λ_{ex} 310); 447 (λ_{ex} 360)	
	solid (298 K)	427 _{max} , 448, 455, 469sh ^c (λ_{ex} 310)	17.6 (λ_{em} 463)
3b	solid (77 K)	463 _{max} , 485, 511 (λ_{ex} 360)	77.0 (λ_{em} 420)
	solid (77 K)	421, 442, 450, 460, 475 (λ_{ex} 300)	34.9 (λ_{em} 460)
3c	CH ₂ Cl ₂ 10 ⁻³ M (298 K)	460 _{max} , 484, 495, 508 (λ_{ex} 360)	
	CH ₂ Cl ₂ 10 ⁻³ M (77 K)	422 (λ_{ex} 360)	
3c	solid (298 K)	438 _{max} , 472sh ^c (λ_{ex} 320)	
	solid (77 K)	446sh, 472 _{max} ^c (λ_{ex} 370)	
3c	solid (298 K)	462 _{max} , 495 ^c (λ_{ex} 360)	
	solid (77 K)	460 _{max} , 485 ^c (λ_{ex} 330)	
3c	CH ₂ Cl ₂ 10 ⁻³ M (298 K)	460, 550 br (λ_{ex} 400)	
	CH ₂ Cl ₂ 10 ⁻³ M (77 K)	407 _{max} , 428sh, 570 _{min} (λ_{ex} 360)	
3c	CH ₂ Cl ₂ 10 ⁻³ M (298 K)	570 (λ_{ex} 405)	
	CH ₂ Cl ₂ 10 ⁻³ M (77 K)	465 _{max} , 547 (λ_{ex} 360)	
3c	CH ₂ Cl ₂ 10 ⁻³ M (298 K)	466 _{min} , 481, 550 _{max} (λ_{ex} 400)	
	CH ₂ Cl ₂ 10 ⁻³ M (77 K)		

^a Data for **1a**: a very weak emission is detected in the solid state at 360 nm (ref 51). ^b A lifetime of 957.8 ns was previously obtained at room temperature using the frequency domain mode. ^c With tail to 600/650 nm. ^d Very weak emission.

Upon photoexcitation, all arylalkynyl complexes (**1–3b,c**) display luminescence in the solid state and in deaerated dichloromethane solutions at 298 K (except **1b**) and at 77 K. The *tert*-butyl derivatives **2a** and **3a** are weakly emissive only at cryogenic temperatures (solid, CH₂Cl₂ glass, 77 K). Complex **1b** shows, both in solid state and in CH₂Cl₂ glass (77 K), a structured band (λ_{max} , 77 K, solid 444 nm; glass 430 nm) with progressional spacing (1132, 2024, 2040 cm⁻¹) typical of a combination of vibrational mode of C≡C and the Ph ring. In accordance with previous assignments in alkynylplatinum complexes^{26,28,34,40,47,50,91–94} and the long measured lifetimes (7.4 μs , 298 K; 48.3 μs , 77 K, solid), the emission is attributed to a spin-forbidden $^3\pi\pi^* \rightarrow ^1\text{GS}$ transition or alternatively to a mixed $^3\text{IL} \pi \rightarrow \pi^*(\text{C}\equiv\text{CPh})/^3\text{MLCT} \text{d}(\text{Pt}) \rightarrow \pi^*(\text{C}\equiv\text{CPh})$ manifold with a predominantly intraligand character. It should be noted that the variation in the wavelength has little influence on the emission spectrum, indicating a single emissive state or multiple states that are in equilibrium. By contrast, complex **1c** exhibits in rigid media (solid, glass 77 K) a structured high-energy emission (i.e., λ_{max} solid 77 K, 451, 472 nm) and one additional broad low-energy emission, which is slightly red-shifted at room temperature (solid 545 nm at 298 K vs 533 nm at 77 K or 523 nm in CH₂Cl₂ glass). The emissions in the solid state (powder) at 77 K are illustrated in Figure 5. As can be seen, the excitation profiles monitored at λ_{em} 452–480 nm and at λ_{em} 530 nm are different, indicating distinct emissive states. It should be noted

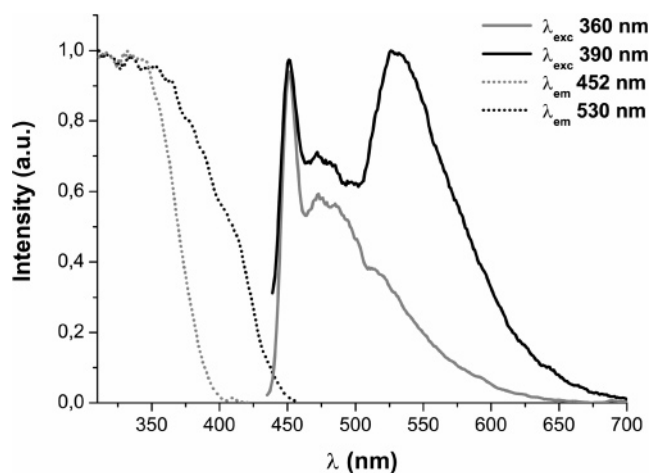


Figure 5. Normalized excitation and emission spectra of **1c** in the solid state (powder) at 77 K.

that the low-energy band is not observed in fluid solution [CH₂Cl₂, 298 K, 427 br; acetone 405sh, 430_{max} (λ_{ex} 360 nm)] and exhibits a clear vibronic profile in acetone glass (Supporting Information, Figure S1). In addition, the measured luminescence lifetimes for both bands (see Table 4) are suggestive of triplet parentage. The observation of dual site-selective emissions in alkynyl complexes is not unprecedented.^{33,50,102} Long-lived dual

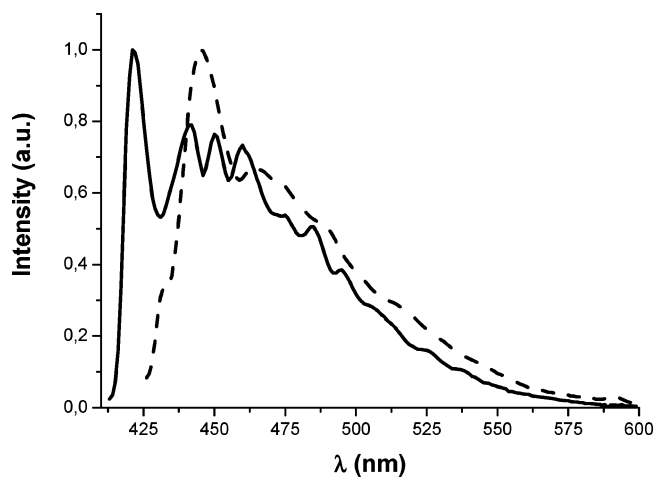


Figure 6. Normalized emission spectra of **2b** (—) and **1b** (---) in the solid state (powder) at 77 K.

emissions have been attributed to ligand-based delayed fluorescence and phosphorescence,⁵⁰ to ligand phosphorescence and exciplex formation with solvent present in the lattice,¹⁰² or to the presence of additional emissive coligands.^{39,103} We also noted that Lukehart, DeGraff, Demas, and co-workers reported¹⁰⁴ that [*trans*-Pt(C≡CR)₂(PEt₃)₂] (R = H, Ph) exhibit site selectivity in their 77 K glass emission spectra, particularly remarkable in the ethynyl derivative, which has been attributed to a ground-state heterogeneity effect.¹⁰⁴ In complex **1c**, the high-energy emission at cryogenic temperatures is comparable to the phosphorescence seen in **1b** or in [*trans*-Pt(C≡CPh)₂(P*n*-Bu₃)₂] (λ_{max} 443 nm, film 77 K)⁹⁴ and the Stokes shift is very large (~ 6000 cm⁻¹), suggesting that it is not delayed fluorescence. A slight wavelength dependence of the emission with excitation wavelength due to the existence of different rotamers involving the C≡CtoI groups (site heterogeneity) could be reasonable, but in complex **1c**, both in solid state and in CH₂Cl₂ glass, the large energy difference between both emissive origins (3678–4190 cm⁻¹) is suggestive of nonequibrated excited states. Thus, although exciplex formation cannot be completely excluded, we suggest that the presence of both emissions could be tentatively attributed to the fact that ³ $\pi\pi^*$ and ³MLCT excited states are not well coupled and their relative energies and decay pathways are presumably affected by the local microenvironment.

For the heterobimetallic complex **2b**, the emission spectra in all media are wavelength independent, indicating again that a single emissive state or several states in equilibrium are responsible for the observed emission. This complex (**2b**) exhibits a well-resolved structure emission (except in room-temperature CH₂Cl₂ solution) with vibrational spacing indicative of the involvement of the C≡CPh ligands in the optical transition. In all media the emission maxima are blue-shifted relative to that observed for the precursor (i.e., solid 77 K 421 nm in **2b** vs 444 nm in **1b**, Figure 6), suggesting, as was commented in the absorption spectra, that the extent of π -conjugation on the alkynyl fragments has decreased upon η^2 -complexation to the CdCl₂ unit. This result is somewhat surprising because bathochromic shifts have been previously observed in other heteropolymetallic η^2 -alkynyl bridging copper

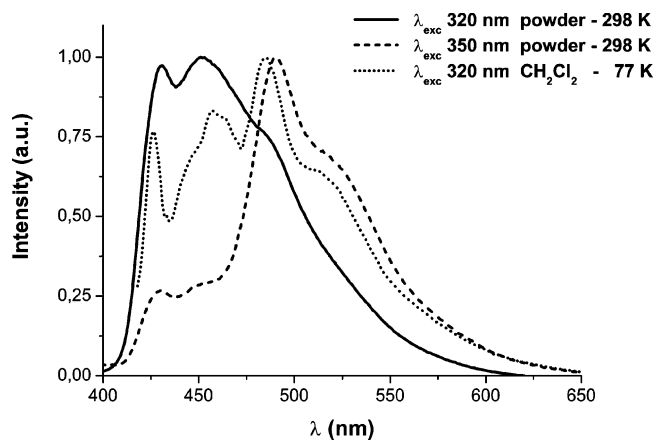


Figure 7. Normalized emission spectra of **2c** in the solid state (powder, 298 K) and in a CH₂Cl₂ 10⁻³ M glass (77 K).

and silver complexes^{40–42,47,50,51,103} and have been attributed to the increased π -accepting ability of the C≡CR groups upon η^2 -coordination. The most significant feature of these Pt–Cd compounds is the absence of Pt \cdots Cd bonding interactions and the fact that the η^2 -complexation takes place in the Pt coordination plane (*in-plane*). *Out-of-plane* π -complexation and weak intermetallic Pt \cdots M or M \cdots M interactions are usually evident in alkynyl platinum–silver and platinum–copper complexes.^{40–42,47,50,51,103} For complexes **2a** and **2c**, multiple emissions are observed. For solid **2a** at 77 K (see Supporting Information, Figure S2) upon excitation at 305 nm, one structured emission with a λ_{max} at 426 nm and a lifetime of 64.2 μ s in this maximum is obtained. On excitation at lower energies (340 and 370 nm), this emission disappears and another structured emission becomes apparent that resembles the overlapping of two bands with λ_{max} starting at 460 and 495 nm, respectively. The measured lifetime in 495 nm fits to two components of 12.4 (73%) and 117.3 μ s (27%), respectively, indicative of spin-forbidden processes. In CH₂Cl₂ glass, the emission is weak and the maxima are similar (see Table 4). As in the precursor, **1c**, a dual emission is observed in the bimetallic complex **2c** in rigid media (see Figure 7) with only slight variations in their maxima (λ_{max} 430, 490 nm solid rt vs 426, 486 nm, CH₂Cl₂ glass). Both the high-energy structured emission resulting from excitation at high energy (λ_{exc} 320 nm) and the low-energy band related to an excitation peak at 350 nm (monitored at λ_{em} 490 nm) are slightly blue-shifted relative to those observed in the precursor (i.e., solid, 298 K, 430 and 490 nm in **2c** vs 454 and 545 nm in **1c**), indicating again that the extent of π conjugation through the alkynyl fragment presumably decreases upon η^2 -complexation to the CdCl₂. In addition, the measured lifetimes in **2c** are longer than in **1c** (see Table 4), suggesting a reduction in the vibrational overlap between the emitting states, tentatively ascribed to ³IL and ³MLCT manifolds, with the ground state. In fluid solution (see Table 4), the low-energy band decreases considerably, appearing only as a shoulder at ca. 493 nm.

At least two close, different emission origins at λ_{max} 430 (λ_{exc} 310 nm) and 447 nm (λ_{exc} 360 nm) are resolved for the trimetallic derivative **3a** in the solid state at 77 K, while the emission profile in CH₂Cl₂ glass exhibits little variation with the wavelength, pointing to ground-state heterogeneity in the solid state.¹⁰⁴ The behavior of complex **3b** is intriguing, differing from that of **1b** and **2b**. Thus, for complex **3b**, the emission is temperature-dependent. At room temperature a greenish-blue emission is observed with maxima at 463, 485, and 511 nm (λ_{exc} 360 nm). The structural spacing of 986 and 2028 cm⁻¹ is

(102) Che, C. M.; Chao, H. Y.; Miskowski, V. M.; Li, Y.; Cheung, K. K. *J. Am. Chem. Soc.* **2001**, *123*, 4985.

(103) Yam, V. W. W.; Yu, K. L.; Wong, K. M. C.; Cheung, K. K. *Organometallics* **2001**, *20*, 721.

(104) Sacksteder, L.; Baralt, E.; Degraff, B. A.; Lukehart, C. M.; Demas, J. N. *Inorg. Chem.* **1991**, *30*, 2468.

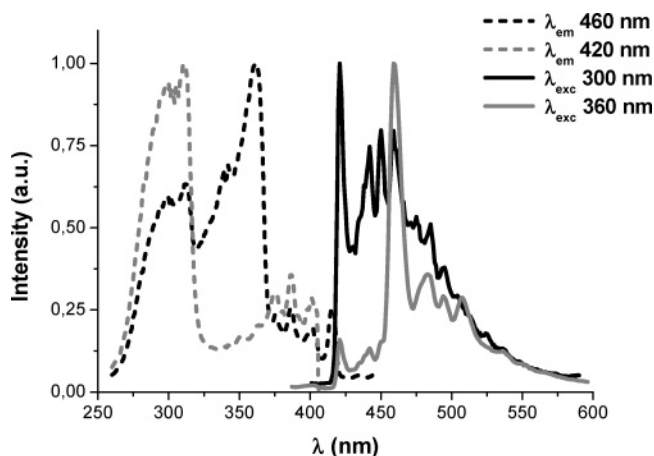


Figure 8. Normalized excitation and emission spectra of **3b** in the solid state (powder) at 77 K.

suggestive of the involvement of the $\text{C}\equiv\text{CPh}$ groups in the optical transition, and its decay fits to only one component (17.6 μs). Upon cooling (see Figure 8), this emission becomes well structured, being mainly observed by excitation at 360 nm. Excitation at shorter wavelengths (300 nm) produces a blue emission showing several vibronic maxima at 421, 442, 450, and 460 nm and several additional low-energy shoulders. Lifetimes of 77 and 34.9 μs were measured for the high- (420 nm) and low-energy (460 nm) emissions, respectively, confirming long-lived, spin-forbidden excited states. As is observed in Figure 8, the corresponding excitation spectra monitored at λ_{em} 420 and 460 nm are clearly different in the 325–370 nm spectral range, suggesting the existence of two closely emitting states. The high-energy band, which is slightly blue-shifted from that seen in **1b** (444 nm, solid 77 K), is assigned to a ${}^3\pi\pi^*$ transition localized on the alkynyl units and the low-energy emission to a ${}^3\text{MLCT}$ or a mixed ${}^3\text{IL}/{}^3\text{MLCT}$ manifold. The absence of the high-energy emission in the solid state at room temperature suggests a very efficient intersystem crossing with the low-energy manifold. Both emissions are also observed in CH_2Cl_2 glass, but slightly red-shifted (λ_{max} 438 and 472 nm, respectively, see Table 4), and only a very weak emission as a broad band centered at 422 nm is obtained upon heating the solution at room temperature.

In the solid state at 298 K, the emission profile of **3c** is similar to that of **3b**, exhibiting, by excitation at 360 nm, a structured low-energy emission with maxima at 462 and 495 nm, respectively. Upon excitation in the 330–360 nm range, the low-temperature (77 K) solid-state spectra are similar to those seen at 298 K (i.e., 460 max., 485 nm λ_{exc} 330 nm). However, on excitation at longer wavelengths (λ_{exc} 400 nm), a broad envelope at 550 nm appears (460 max., 550 nm broad), suggesting the existence of two low-lying energy-emitting states. Both emissions are slightly red-shifted from those seen in the precursor complex **1c** (solid 77 K, 451 and 533 nm) and very well resolved in CH_2Cl_2 glass (see Figure 9 and Table 4). It is interesting to note that in CH_2Cl_2 solution (298 K) complexation of both dianionic fragments $[\text{Pt}(\text{C}_6\text{F}_5)_2(\text{C}\equiv\text{CTol})_2]^{2-}$ to Cd^{2+} switch on a low-energy emission (570 nm) (Supporting Information, Figure S3), which is not observed in CH_2Cl_2 for the precursor **1c** at 298 K. The high-energy emission (407, 428 nm) appears at a similar energy as in **1c** (427 nm) and is related to an excitation peak at 373 nm, while the excitation spectrum monitored at 570 nm shows a prominent peak at 404 nm with a shoulder at 373 nm (Supporting Information, Figure S3). These emissions are tentatively ascribed, as in the precursor, to ${}^3\pi\pi^*$

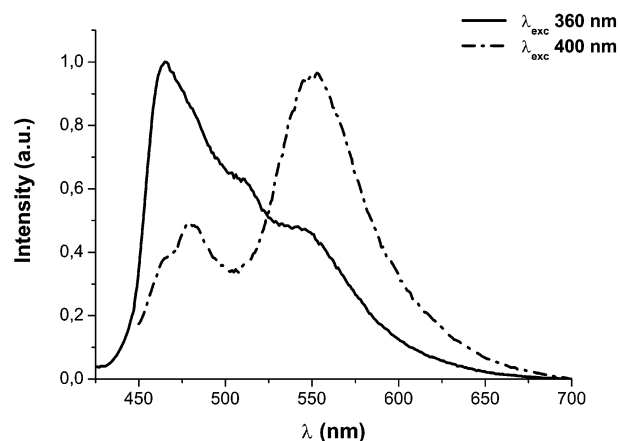


Figure 9. Normalized emission spectra of **3c** in CH_2Cl_2 (10^{-3} M) glasses (77 K).

and ${}^3\text{MLCT}$ (or mixed ${}^3\pi\pi^*/{}^3\text{MLCT}$) transitions, respectively. The structureless profile of the low-energy emission and its remarkable rigidochromism (CH_2Cl_2 570 nm, 298 K vs 550 nm, 77 K) is supportive of a more MLCT character.

Summary

Two series of hetero bi- and trimetallic tweezer-type complexes $[\{cis\text{-Pt}(\text{C}_6\text{F}_5)_2(\text{C}\equiv\text{CR})_2\}\text{CdCl}_2]^{2-}$ (**2**) and $[\{cis\text{-Pt}(\text{C}_6\text{F}_5)_2(\text{C}\equiv\text{CR})_2\}_2\text{Cd}]^{2-}$ (**3**), stabilized by η^2 -alkyne–cadmium bonds ($\text{R} = t\text{-Bu}$ **a**, Ph **b**, Tol **c**), have been synthesized and characterized. Crystal X-ray structures of **2c** and **3a,b** confirm that in all cases the cadmium center is well embedded by the *cis*-bis(alkynyl)platinate entity, leading to planar $\text{Pt}(\text{C}\equiv\text{C})_2\text{Cd}$ cores. Complexes **3** are the first reported examples in which a Cd^{2+} ion is stabilized only by four η^2 -alkyne interactions. The photophysical properties of the precursors **1** and the novel alkynyl bridging heterometallic species (**2**, **3**) have been examined. The incorporation of CdCl_2 (**2**) or Cd^{2+} (**3**) by η^2 -alkyne interactions to **1** causes hypsochromic shifts in the low-energy absorptions, which has been attributed to the existence of a lesser electron delocalization on the alkynyl fragments upon η^2 -complexation. The emissive properties of these complexes have been examined. Structured emission bands are usually observed and are believed to arise from ${}^3\pi\pi^*(\text{C}\equiv\text{CR})$ (IL) and/or mixed ${}^3\pi\pi^*/\text{Pt}(\text{d}_\pi)(\text{C}\equiv\text{CR}) \rightarrow \pi^*(\text{C}\equiv\text{CR})$ (${}^3\text{MLCT}$) manifolds with a predominant IL character. For the tolyl alkynyl derivatives **1c–3c** dual emissions are observed in rigid media, which are tentatively attributed to the fact that ${}^3\pi\pi^*$ and ${}^3\text{MLCT}$ (or mixed ${}^3\pi\pi^*/{}^3\text{MLCT}$) excited states are not coupled. For the trimetallic derivative **3c** dual emission is observed even in fluid solution. In the case of phenylethynyl complexes (**1b–3b**) a similar behavior (dual-emission) is observed only for the trimetallic derivative **3b** at 77 K, suggesting effective coupling of ${}^3\pi\pi^*$ IL/ ${}^3\text{MLCT}$ manifolds for **1b** and **2b** (298, 77 K) and also for **3b** at 298 K. The *tert*-butylalkynyl derivatives **2a** and **3a** are only weakly emissive at 77 K, and the profiles of emission spectra exhibit a slight dependence with excitation wavelength, which is believed to arise from ground-state heterogeneity.

Acknowledgment. This work was supported by the Spanish Ministry of Science and Technology (Projects BQU2002-03997-C02-01, 02 and CTQ2005-08606-C02-01, 02). B.G. wishes to thank the CSIC for a grant.

Supporting Information Available: Figures S1–S3. Crystallographic data in CIF format. This material is available free of charge via the Internet at <http://pubs.acs.org>.

OM051094U